An-Najah National University
Faculty of Graduate Studies

First Principle Electronic Structure Calculations of Ternary alloys. BN_xP_{1-x}, Ga_xB_{1-x} N and B_xIn_{1-x} N in zinc blende structure

By
Baseemeh Daas Fareed Zpeedeh

Supervisor
Dr. Musa El-Hasan
Dr. Rezek M. Estaiteh

Submitted in partial fulfillment of the requirements For the degree of Master of Science in physics An-Najah National University, Nablus - Palestine
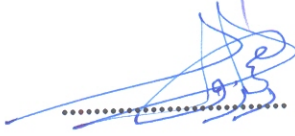
2008

First Principle Electronic Structure Calculations of Ternary alloys. BN_xP_{1-x}, $Ga_xB_{1-x} N$ and $B_xIn_{1-x} N$ in zinc blende structure

By

Baseemeh Daas Fareed Zpeedeh

This thesis was defended successfully on 27/8/2008, and approved by

Committee Members		Signature
1- Dr.Musa El-Hasan	(Supervisor)	
Assistant Professor		
2- Dr. Rezek Estaiteh	(Co-Supervisor)	
Assistant Professor		
3- Dr. Mohammed Abu- Jafar	(Internal Examiner)	
Associate Professor of Physics		
4- Dr. Marwan El- Koni	(External Examiner)	
Associate Professor of Physics		

ACKNOWLEDGMENTS

I would like to express my sincere feelings to my supervisor, Prof. Dr. Musa El-Hasan and Dr. Rezek Estaiteh. I am grateful for their painstaking care in the course of this project, for their meticulous effort in teaching me very precious, numerous concepts. I could have done nothing without them. I would like to thank also my parents, all the members of my family, and all the teachers in the physics department and in school for their endless help during my study. Finally, there is no words that can describe these people in for their generosity and kindness which I saw and felt during my study in this university.

<div dir="rtl">

الإقرار

أنا الموقع أدناه مقدم الرسالة التي تحمل العنوان:

</div>

First Principle Electronic Structure Calculations of Ternary alloys. BN_xP_{1-x}, Ga_xB_{1-x} N and B_xIn_{1-x} N in zinc blende structure

<div dir="rtl">

أقر بأن ما اشتملت عليه هذه الرسالة انما هي نتاج جهدي الخاص   باستثناء ما تمــت الاشارة اليه حيثما ورد   وأن هذه الرسالة ككل   أو أي جزء منها لم يقدم من قبل لنيــل أيــة درجة علمية أو بحث علمي أو بحثي لدى أية مؤسسة تعليمية أو بحثية أخرى.

</div>

Declaration

The work provided in this thesis, unless otherwise referenced, is the researcher's own work, and has not been submitted elsewhere for any other degree or qualification.

Student's name:	اسم الطالب:
Signature:	التوقيع:
Date:	التاريخ:

TABLE OF CONTENTS

LIST OF TABLES

LIST OF FIGURES

First Principle Electronic Structure Calculations of Ternary alloys.
BN_xP_{1-x}, Ga_xB_{1-x} N and B_xIn_{1-x} N in zinc blende structure
By
Baseemeh Daas Fareed Zpeedeh
Supervisor
Dr. Musa El-Hasan
Dr. Rezek M. Estaiteh

Abstract

In this work full-potential linearized augmented plane wave method (FP-LAPW) within the density functional theory (DFT) and within generalized gradient approximation (GGA) are used to investigate, electronic band structure, structural properties and thermodynamic properties of III (In, B, Ga) - V (N, P) compounds and their ternary alloys of BN_xP_{1-x}, $Ga_xB_{1-x}N$, $B_xIn_{1-x}N$ in zinc blende structure.

The present DFT-GGA calculations have shown direct band gap energy in zinc-blende phase for InN, GaN, and indirect band gap energy for BN and BP. Here, the conduction band minima of both InN and GaN are located at Γ point, while that of BN is at a position lying along Γ–X direction and BP at Γ–Δ_{min} .

In our work we have found that the band gap engineering of BN_xP_{1-x}, $Ga_xB_{1-x}N$, $B_xIn_{1-x}N$ alloys have been studied for range of constituents (x= 0.25, 0.50, 0.75). The downward band gap bowing seems the largest in $Ga_xB_{1-x}N$ alloy comparable with the other alloys considered in this work. Even for a small amount of contents (x), adecrease of the electronic effective mass around Γ point appears for BN_xP_{1-x}, $Ga_xB_{1-x}N$, $B_xIn_{1-x}N$ alloys manifesting itself by an increase of the band curvature .

The calculated cross over from indirect to direct band gap of ternary alloys has been found to be consistent with the experimental measurements.

At last, the determinations of the band gaps of alloys as a function of contents, the concentration range of constituents leading to metallic character of the alloys, the change of the electronic effective mass around (Γ) as a function of the cross over from indirect to direct band gap of the alloys which are direct on one end, indirect on the other end are main achievements in this work.

We have found also that the optimize volume and the thermo-dynamic properties were different with different concentrations of the component of their ternary alloys above and we have also analyzed the relative stability, the bulk modulus, and the minimized energy of these ternary compounds.

CHAPTER ONE

INTRODUCTION

semiconductors can be grown with varying compositions. Also the quality of materials was improved which increases the possibility of applications. The III nitride (GaN, BN, InN) and BP semiconductors are potentially useful at high frequency, microwave and short-wave-length.

InN, and GaN are used for high speed hetero junction transistors [1] and low cost solar cells with high efficiency [2]. They are also increasingly used for visible light emitting diodes (LEDs) [3, 4] and laser diodes (LDs) [5-8], for the amber, green, blue and UV regions of the spectrum. Also as basis for high power, high temperature electronic devices [9, 10].

It is well known that InN has the smallest energy gap of any of the III-V binary materials used, which makes it an interesting narrow gap semiconductor, from the point of view of optical spectroscopy and optoelectronic applications [11]. This property often allows the fabrication of infrared imaging systems, free space communications, and gas phase detection systems [12,13]. BN has a largest electronic band gap a mong III-V compounds which has a particular importance for optoelectronic devices. Optoelectronic devices can be designed so that to cover a wide spectral range.

In our work DFT was used to calculate energy gap of the ternary alloys BN_xP_{1-x}, $Ga_xB_{1-x}N$, and $B_xIn_{1-x}N$, and the physical properties of these alloys.

The ternary alloys of $Ga_xB_{1-x}N$, $B_xIn_{1-x}N$, and BN_xP_{1-x} are the potential materials for room temperature infrared detectors, gas sensors and lasers operating in near infrared (0.9-1.3 µm), mid - infrared (2-5 µm) and far infrared (8- 12 µm) regions[14–23]. Also they have applications as a cladding layer or an active layer for light emitting diodes LEDs and laser diodes LDs emitting an extremely wide spectral region covering from deep ultraviolet (UV) to infrared [24] and as a potential material for thermo electric power devices [25], solar cells with high efficiency [26], buffer layer for multiple quantum lasers [27] .

The theoretical methods which can be used to study the properties of exotic semiconductors for this can be classified according to the input data:

● **First principles calculation (ab-initio calculations)**. In these kinds of calculations only the atomic number and the number of the atoms are used as an input for the calculations. Full potential linearized augmented plane wave (FP-LAPW) method based on (DFT) within (LDA) [28, 29] or (GGA) [28–30], and Hatree- Fock [31] method are used as first principle calculation methods in the literature.

● **Empirical methods:** These kinds of calculational methods needs interaction energy parameters which are externally obtained from either

experimental measurements or the first principles calculation results. The $\vec{k}.\vec{p}$ [32, 33], empirical pseudo potential (EPP) [34] and empirical tight binding (ETB) [35, 36] are used as empirical methods in the literature.

In the present work, FP-LAPW method within GGA is applied on InN, GaN, BP and BN compounds and their ternary alloys to find out the electronic band structure for these materials. Because of the time consuming problem in the first principle calculations of alloys, DFT method is mainly used in the present work to study the band bowing of BN_xP_{1-x}, $Ga_xB_{1-x}N$, and $B_xIn_{1-x}N$ alloys.

This thesis is organized as follows: In chapter 2, the calculation methods used in this work are explained and formulated. In chapter 3 the electronic band structure for InN, GaN, BP and BN has been studied, respectively. In chapter 4 the band gap bowing BN_xP_{1-x}, $Ga_xB_{1-x}N$, and $B_xIn_{1-x}N$ alloys has been studied respectively. Finally, the results will be discussed and conclusions will be drawn.

CHAPTER TWO
THEORY OF CALCULATION

2-1 Introduction:

Nowadays atomistic and electronic structure calculations have become very important in the fields of physics and chemistry than the past decade, especially with the high-performance computers. If we need to know the atomic structure of the material, electronic properties and how can we modify the bonding between atoms or the material chemical content to create new materials with properties different from original properties of the component.

A number of methods can be used. It can be divided into two classes: those that do not use any empirically or experimentally derived quantities called first principles methods, like density functional theory (DFT), while the latter methods are called empirical or semi-empirical, like empirical tight binding (ETB). The first principle methods are useful in predicting the properties of new materials such as the calculation of the energy levels of electrons in solids, which used to know the energy bands, which is the central theoretical problem of solid state physics. Knowledge of these energies, and electron wave function is required for any calculation of more directly observable properties including electrical and thermal conductivities, optical dielectric function, vibration spectra and so on.

In the present work, the energy band structure of compounds, such as InN, BN, BP, GaN and their ternary alloys BN_xP_{1-x}, $Ga_xB_{1-x}N$, and B_xIn_{1-}

$_x$N has been obtained by the combination of first principle calculations based on density functional theory.

The theory of the calculation considered in this work has been outlined in the following section

2.2 Density Functional Theory as a way to solve the quantum many body problem

A solid is a collection of heavy, positively charged particles (nuclei), If the structure is composed of N nuclei and each has Z electrons, then it has N (nuclei) + Z N (electrons) electromagnetically interacting particles. This is known as a many-body problem, and because these particles are so light compared with classical scale, it is a quantum many body problem. In principle, to study the materials and their properties, the theorist has to solve the time independent Schr dinger equation.

$$\hat{H}\ \Psi\ =\ E\Psi \tag{2.1}$$

where

$$H = T_n + T_e + V_{en} + V_{ee} + V_{nn} \tag{2.2}$$

$$\hat{H} = -\frac{\eta^2}{2}\sum_i \frac{\nabla^2_{Ri}}{M_i} - \frac{\eta^2}{2}\sum_i \frac{\nabla^2_{ri}}{m_e} - \frac{1}{4\pi\varepsilon_o}\sum_{i,j}\frac{e^2 Z_i}{\left|R_i - r_j\right|}$$
$$+ \frac{1}{8\pi\varepsilon_o}\sum_{i \neq j}\frac{e^2}{\left|r_i - r_j\right|} + \frac{1}{8\pi\varepsilon_o}\sum_{i \neq j}\frac{e^2 Z_i Z_j}{\left|R_i - R_j\right|} \tag{2.3}$$

Here Ψ, is the wave function of all participating particles and H is the exact many-particle Hamiltonian for this system. The first term in equation (2.3)

is the kinetic energy operator for the nuclei (T_n), the second for the electrons (T_e). The third term corresponds to Coulomb electron-nuclear attraction (V_{en}), the forth term for electron-electron repulsion (V_{ee}) and the final term for nuclear-nuclear repulsion (V_{nn}), respectively M_i is the mass of the nucleus at R_i, m_e is the mass of the electron at r_i. In order to find acceptable approximate eigenstates (acceptable solution to Schr dinger equation (2.1)), three approximations at different levels can be used.

These approximations make the calculations easy to transform the many body problem to one body problem.

2.2.1 Level 1: The Born-Oppenheimer approximation (BO)

One of the most important approximations in material science. The special idea of the approximation is that the nuclei are much heavier and much slower than the electrons. We can hence` freeze' them at fixed positions and assume the electrons to be in instantaneous equilibrium with them. This mean that only the electrons are kept as players in this many body problems while nuclei are deprived from this status, and reduced to a given source of positive charge; they become 'external' to the electron cloud.

The application of this approximation; left the problem with a collection of ZN interacting negative particles, moving in the (now external or given) potential of the nuclei. So the consequences of the Born-Oppenheimer approximation of the Hamiltonian the nuclei do not move

any more, their kinetic energy is zero and the first term in equation (2.2) disappears and the last term reduces to a constant. Therefore the many body problem is left with the kinetic energy of the electron gas, the potential energy due to electron- electron interactions and the potential energy of the electrons in the (now external) potential of the nuclei. The new many body Hamiltonian is written formally as

$$\hat{H} = -\frac{\eta^2}{2} \sum_i \frac{\nabla_{ri}^2}{m_e} + \frac{1}{8\pi\varepsilon_o} \sum_{i\neq j} \frac{e^2}{|r_i - r_j|} - \frac{1}{4\pi\varepsilon_o} \sum_{i,j} \frac{e^2 Z_i}{|R_i - r_j|}$$

Or

$$H = T_e + V_{ee} + V_{ext} \tag{2.4}$$

2.2.2 Level 2: Density Functional theory (DFT)

The quantum many body problem obtained after the first level approximation (Born-Oppenheimer) is much simpler than the original one, but still difficult to solve. To reduce equation 2.4 to an approximate but acceptable form the Hartree-Fock method (HF) is needed. In this approximation [37], the solution of many-electron Hamiltonian is transformed to solve one-electron Hamiltonian by assuming the electrons are independent from each other. By this assumption the total wave function for the electrons is written as

$$\Psi(r_1, r_2,\dots\dots .r_N) = \prod_i^N \psi(r_i) \tag{2.5}$$

Where(Ψ) is the electron wave function. Using this definition

$$\rho(r) = \sum_i^N |\psi_i(r)|^2 \tag{2.6}$$

Where ($\rho(r)$) is the electron density

The total Hamiltonian can be written

$$\hat{H} = -\frac{\eta^2}{2m_e}\sum_i \nabla_{ri}^2 - \frac{1}{4\pi\varepsilon_o}\sum_i \sum_j \int \frac{eZ_j|\psi(r_i)|^2 d^3r_i}{|R_j - ri|}$$
$$+ \frac{1}{8\pi\varepsilon_o}\sum_i \sum_j \frac{|\psi(r_i)|^2|\psi(r_j)|^2 d^3r_j d^3r_i}{|r_i - r_j|}$$

Or

$$H = T_0 + V_H(\psi) \tag{2.7}$$

The Schr dinger equation becomes non-linear and requires for the

Self consistency procedure.

$$[T_o + V_H(\psi)]\Psi = E_H\Psi \tag{2.8}$$

Here, T_0 is the functional for the kinetic energy of a non-interacting electron gas, V_H stands for the electron effective potential and E_H is the functional of electron energy using Hartree approximation. In order to solve an equation of this type, one starts with some trivial solution $\Psi^{(o)}$ (normally atomic orbital wave function is used) which

is used to construct the potential.

Solving the nonlinear Schr dinger equation (2.8) with this potential, one can obtain a new solution $\Psi^{(1)}$ which is used in turn to build a new potential. This procedure is repeated until the ground state $\Psi^{(i)}$ and the

corresponding energy E do not deviate appreciably from those in the previous step.

Hartree product wave functions suffer from several major flaws that serve to make them physically unrealistic:

- Hartree products do not satisfy the Pauli anti symmetry principle this means that the sign of any many-electron wave function must be anti symmetric with respect to the interchange of the coordinates, both space and spin, of any two electrons. The anti symmetry principle is a postulate of quantum mechanics. The Pauli principle prevents two electrons with the same spin from occupying the same spatial orbital.

- Hartree product force a particular electron to occupy a given spin orbital despite the fact that electrons are indistinguishable from one another. Lastly, because the Hartree product wave function is constructed on the assumption that the electrons are non-interacting, there exists a non-zero probability of finding two electrons occupying the exact same point in space.

Later this wave function is modified to include the spin of the electron by the Hartree-Fock approximation [38]. This approximation is an extension of the above Hartree approximation, to include the permutation symmetry of the wave function which leads to the exchange interaction. Exchange is due to the Pauli exclusion principle, which states that the total wave function for the system must be anti symmetric under particle exchange.

This means that when two arguments are swapped the wave function

changes sign as follows:

$$\Psi(r_1, r_2, r_i, r_j, \ldots \ldots r_N) = -\Psi(r_1, r_2, r_j, r_i, \ldots \ldots r_N) \tag{2.9}$$

Where r_i includes coordinates of position and spin. Therefore no two electrons can have the same set of quantum numbers, and electrons with the same spin cannot occupy the same state simultaneously.

As a result of the anti symmetry wave function, eq (2.8) can be written as

$$E_{HF} = T_o + V_H \tag{2.10}$$

E_{HF} is the functional electron energy using Hartree-Fock

approximation, T_o is the functional for the kinetic energy of a non-interacting electron gas and V_H stands for the electron effective potential. The solution steps of eq.(2.10) are the same as they are defined for Hartree eq.(2.7). Hartree-Fock approximation performs very well for atoms and molecules, and therefore used a lot in quantum chemistry. For solids it is less accurate, however. In the present work, the electronic band structure of compounds and ternary alloys has been studied by DFT which is more modern and probably more powerful compared to HF approximation. Density Functional Theory formally established in 1964 by two theorems due to Hohenberg and Kohn [39].

2.2.3 The theorems of Hohenberg and Kohn

The traditional formulation of the two theorems of Hohenberg and Kohn is as follows:

- **First theorem**: their is one-to-one correspondence between ground-state density of a many-electron system (atom, molecule, solid) and the external potential V_{ext}. An immediate consequence is that the ground-state expectation value of any observable quantity,

is a unique functional of the exact ground-state electron density

$$\langle \Psi | O | \Psi \rangle = O(\rho) \qquad (2.11)$$

From this wave function, the corresponding electron density is easily found.

- **Second theorem**: For O being the Hamiltonian H, the ground- state total energy functional is of the form

$$E_{Vext}[\rho] = \langle \Psi | T + V | \Psi \rangle + \langle \Psi | V_{ext} | \Psi \rangle \qquad (2.12)$$

or

$$E_{vext}[\rho] = F_{HK}[\rho] + \int \rho(r) V_{ext}(r) dr \qquad (2.13)$$

Where the Hohenberg-Kohn density functional $F_{HK}[\rho]$ is universal for any many-electron system.

E_{Vext} [ρ] reaches its minimal value   for the ground state density corresponding to V_{ext}.

Now its important to discuss the meaning of the following keywords.

- **First, the Invariability:** It is obvious that a given many electron system has a unique external potential, which by the Hamiltonian 2.1 and the Schr dinger equation yields a unique ground-state many particle wave function. From this wave function, the corresponding electron density is easily found. An external potential hence leads to a unique ground-state density corresponding to it. But it looks like the density contains less information than the wave function. If this would be true, it would not be possible to find a unique external potential if only a ground-state density is given.

   The first theorem of Hohenberg and Kohn tells exactly that this is possible.

   The density contains as much information as the wave function does (i.e. every thing you could possibly know about an atom, molecule or solid). All observable quantities can be written as functional of the density.

- **Universality (the universality of $F_{HK}[ρ]$):** Eq. 2.13 is easily

written down by using the density operator, and supposing the ground-state density is known, the contribution to the total energy from the external potential can be exactly calculated.

An explicit expression for the Hohenberg-Kohn functional, F_{HK}, is not known. But anyway, because F_{HK} does not contain information on the nuclei and their position, it is a universal functional for any many- electron system.

This means that in principle an expression for $F_{HK}[\rho]$ exists which can be used for every atom, molecule or solid which can be imagined.

• **variation access**: the second theorem makes it possible to use the variation principle of Rayleigh-Ritz in order to find the ground-state density. Out of the infinite number of possible densities, the one which minimizes $E_{V_{ext}}[\rho]$ is the ground-state density corresponding to the external potential $V_{ext}(r)$. Of course, this can be done only if (an approximation to) $F_{HK}[\rho]$ is known. But having found ρ, all knowledge about the system is known. When it is evaluated for the ρ density corresponding to the particular V_{ext} for this solid, it gives the ground state energy. When it is evaluated for any other density however, the resulting number has no physical meaning.

The practical procedure to obtain the ground state density of DFT was satisfied by Kohn and Sham equation published in 1965 [40]. In Kohn Sham equation, the correlation energy (V_c): is this part of the total energy which is present in the exact solution, but absent in the Hartree-Fock solution.

The total energy functional E_e corresponding to the exact Hamiltonian

$$E_e = T + V \tag{2.14}$$

and $E_{HF}[\rho]$ corresponding to the Hartree-Fock Hamiltonian

$$E_{HF} = T_o + (V_H + V_x) \tag{2.15}$$

Here T is the exact kinetic energy and V electron-electron potential energy functionals, T_o is the functional for the kinetic energy of a non interacting electron gas, V_H stands for the Hartree contribution and V_x for the exchange contribution. By subtracting equation (2.15) from equation (2.14), the functional for the correlation contribution appears to be

$$V_c = T - T_o \tag{2.16}$$

The exchange contribution to the total energy is defined as the part which is present in the Hartree-Fock solution, but absent in the Hartree solution.

The Hartree functional given by

$$E_H = T_o + V_H \tag{2.17}$$

It can be defined as

$$V_x = V - V_H \tag{2.18}$$

With this knowledge, we can rewrite the Hohenberg-Kohn functional in the following way

$$F_{HK} = T + V + T_o - T_o \qquad (2.19)$$

$$= T_o + V + (T - T_o) \qquad (2.20)$$

Where from equation (2.16) $T - T_o = V_c$

$$F_{HK} = T_o + V + V_c + V_H - V_H \qquad (2.21)$$

$$= T_o + V_H + V_c + (V - V_H) \qquad (2.22)$$

Where from equation (2.18) $V - V_H = V_x$

$$F_{HK} = T_o + V_H + (V_x + V_c) \qquad (2.23)$$

Here (V_{xc}) is the exchange-correlation energy functional which we don't know it formally, as it contains the difficult exchange and correlation contributions only. If we assume for a while that we do know V_{xc}, we can write explicitly the energy functional:

$$E_{Vext}[\rho] = T_0[\rho] + V_H[\rho] + V_{xc}[\rho] + V_{ext}[\rho] \qquad (2.24)$$

One could use now the second Hohenberg-Kohn theorem to find the ground state density, but instead, one can interpret the above expression also as the energy functional of a non-interacting classical electron gas, subject to two external potentials: one due to the nuclei, and one due to exchange and correlation effects. The corresponding Hamiltonian (called the Kohn-Sham Hamiltonian) is

$$H_{KS}=T_o+ V_H+ V_{xc} +V_{ext} \tag{2.25}$$

Or

$$H_{KS} = -\frac{\eta^2}{2m_e}\nabla_i^2 + \frac{e^2}{4\pi\varepsilon_o}\int\frac{\rho(r_i)}{|r-r_i|}dr + V_{xc} + V_{ext} \tag{2.26}$$

Where, the exchange-correlation potential is given by the functional

derivative

$$\hat{V}_{xc} = \frac{\delta V_{xc}(\rho)}{\delta(\rho)} \tag{2.27}$$

2.2.4 The Kohn-Sham equations:

The theorem of Kohn and Sham can be formulated as follows: The exact ground-state density $\rho(r)$ of an N-electron system is

$$\rho(r) = \sum_{i=1}^{N} \Psi_i^*(r)\Psi_i(r) \tag{2.28}$$

Where, the single-particle wave functions $\Psi_i(r)$ are the N lowest-energy Solutions of the Kohn-Sham equation

$$H_{KS}\Psi_i = E_i\Psi_i \tag{2.29}$$

And now, we did won a lot. To find the ground-state density, we don't need to use the second Hohenberg-Kohn theorem any more, but we can rely on solving the familiar Schr dinger (like non interacting single particle) equations. But be aware that the single-particle wave functions, Ψ_i (r), are not the wave functions of electrons, they describe mathematical

quasi-particles, without a direct physical meaning. Only the overall density of these quasi- particles is used to be equal to the true electron density. Also the single particle energies, E_i are not single-electron energies. Both the Hartree operator V_H and the exchange-correlation operator V_{xc} depend on the density $\rho(r)$, which in turn depends on the $\Psi_i(r)$ which are being searched.

Some starting density $\rho(o)$ is guessed, and a Hamiltonian H_{KS1} is constructed with it. The eigenvalue problem is solved, and results in a set of Ψ_i from which a density ρ_1 can be derived. Most probably ρ_o will differ from ρ_1. Now ρ_1 is used to construct H_{KS2}, which will yield a ρ_2, etc. The procedure can be set up in such a way that this series will converge to a density ρ_f which generates a H_{KSf} which yields as solution again ρ_f, this final density is then consistent with the Hamiltonian.

2.2.5 The exchange-correlation functional:

The Kohn-Sham scheme described above was exact: apart from the preceding Born-Oppenheimer approximation, no other approximations were made. But we neglected so far the fact that we do not know the exchange-correlation functional. It is here that approximations enter this theory.

A widely used approximation called the Local Density Approximation (LDA) is to postulate that the exchange-correlation functional has the following form

$$E_{xc}^{LDA} = \int \rho(r)\varepsilon_{xc}(\rho(r))dr \qquad\qquad (2.30)$$

This postulate is somehow reasonable; it means that the exchange-correlation energy due to a particular density ρ (r) could be found by dividing the material in infinitesimally small volumes with a constant density.

Each such volume contributes to the total exchange correlation energy by an amount equal to the exchange correlation energy of an identical volume filled with a homogeneous electron gas, which has the same overall density as the original material has in this volume.

A next logical step to improve on LDA is to make the exchange-correlation contribution of every infinitesimal volume not only dependent on the local density in that volume, but also on the density in the neighboring volumes. In other words, the gradient of the density will play a role. This approximation is therefore called the Generalized Gradient Approximation (GGA). There is only one LDA exchange-correlation functional, because there is a unique definition for exchange-correlation. But therefore several versions of GGA exist. Moreover, in practice one often fits a GGA-functional with free parameters to a large set of experimental data on atoms and molecules.

The best values of these parameters are fixed , and the functional is ready to be used routinely in solids. Therefore such a GGA-calculation is strictly in calculation. Nevertheless, there exist GGA's that are parameter free.

2.2.6 Level 3: Solving the equations

Solving an infinite set of one-electron equations of the following type:

$$\left(\frac{-\eta^2}{2m_e}\overrightarrow{\nabla_m^2}+\frac{e^2}{4\pi\varepsilon_o}\int\frac{\rho(r')}{|r-r'|}dr'+V_\alpha+V_{ext}\right)\Psi_m(r)=\varepsilon_m\Psi_m(r) \qquad (2.31)$$

Here, m is an integer number that counts the members of the set, the term $\left(\frac{-\eta^2}{2m_e}\overrightarrow{\nabla_m^2}+\frac{e^2}{4\pi\varepsilon_o}\int\frac{\rho(r')}{|r-r'|}dr'+V_\alpha+V_{ext}\right)$ was called H_{sp} the single-particle Hamiltonian. For HF, $V_{\acute{\alpha}}$ is the exchange operator.

The Ψ_m are true one-electron or single particle orbital for HF. Exchange is treated exactly, but correlation effects are not included at all. For DFT, $V_{\acute{\alpha}}$ is the exchange-correlation operator, in the local spin density approximation (LSDA), GGA or another approximation. Exchange and correlation are both treated, but approximately. The Ψ_m are mathematical single-particle orbital.

The similarity between the Hartree-Fock and Kohn-Sham equations means that the same mathematical techniques can be used to solve them.

CHAPTER THREE
THE RESULTS AND DISCUSION OF InN, GaN, BN AND BP COMPOUNDS

3.1 Introduction

Recently there has been increasing interest to study wide band gap semiconductors. There are several reasons for this interest: these materials are required for high temperature applications and for photoelectronic applications in the short wave length range of the visible spectrum and near UV.

III-V compounds such as Boron, gallium with nitrogen have wide band gap. The reason for the wide band gap of these materials are due to the strong covalent interaction. Their bonding is manifested in their high cohesive energies, strong elastic constant, and the hardness's. This makes them useful for reinforcement in metal- ceramic and ceramic- ceramic composites.

The narrow band gap compounds such as Indium with Nitrogenand Boron with phosphor have also attract researchers to study because of its optical and high temperature device applications. The physical properties of InN have attracted considerable research interest because of its transport properties such as high electron mobility and saturation velocity making InN a promising candidate for use in high-speed devices. In addition, InN and GaN alloys and hetero structures will enable unique optoelectronic devices, operating from near infrared to ultraviolet wavelength. However, the range of device applications strongly depends on the material

properties, quality, and on the extent to which indium-rich alloys and hetero structures can be formed.

Among these InN is used for the fabrication of high speed hetero-junction transistors [1] and low cost solar cells with high efficiency [2] because of a highly potential material. Pure InN was predicted to have the lowest effective mass for electrons in all the III-nitride semiconductors [1] which lead to high mobility.

Recently, several groups have grown high quality hexagonal (w-InN) and zinc-blende (c-InN) structural InN films by modern growth techniques, such as metal organic chemical vapor deposition (MOVP E) and plasma-assisted molecular beam epitaxy (MBE) [41-46]. The w-InN and c-InN films have been mostly grown on sapphire. The LDA calculations that employed the pseudopotential (PP) method produced negative band gaps ranging from -0.18 to -0.40 eV [47- 52]. The GGA within the (PP) led to a gap value of -0.55eV [49]. The recent experiment works on c-InN have mainly focused on the characterization of the films [43-46]. The band gap energy of c-InN films has not been reported experimentally according to our knowledge, but it has been found around 0.44 - 0.74 eV by the results of ab-initio-calculations [53,54]. These newly reported values of w-InN and c-InN are compatible with the wavelength of the optical fiber. Therefore, the w-InN and c-InN films will have very important potential to fabricate high speed laser diodes (LDs) and photodiodes (PDs) in the optical communication systems.

The other compound of N, GaN it is used for microelectronic and optoelectronic applications. In GaN multi-quantum well light emitting diodes (LEDs) within tin oxide as widow layers were fabricated with the band gap of 3.1 - 3.5 eV is a very useful material for a large range of applications, such as emitters and detectors for visible and UV light, for high frequency, high temperature and power devices [6, 55-57]. The stable GaN has been grown in hexagonal (wurtzite phase) structure. However, the production of GaN thin films of cubic (c) (zinc-blende phase) crystals has been satisfied by the recent progress in crystal growth techniques.

Recently, the high quality pure c-GaN epilayers have been successfully grown on by gas phase and plasma assisted molecular beam epitaxy (MBE) [58-69] and metal organic chemical vapor deposition (MOCVD) [66,68].

The interest in c-GaN has been growing recently. Because the c-GaN has some attractive advantages for device applications such as higher electron drift velocity [67] and lower band gap energy than w-GaN [53-64,66]. The band gap of c-GaN was calculated to be 1.6 eV by pseudopotential Gaussian basis (LDA/PP-GB) [70], 1.89 eV by pseudopotential plane-wave (LDA/PPPW) [71], 1.28 eV by GGA/PPPW [72] and 2 eV by all-electron (LDA/AE) [73].

In the literature, there are large theoretical efforts to describe the structural and electronic properties of c-GaN [62, 74- 88]. The direct band gap values by density functional theory (DFT) within local density

approximation (LDA) were found to be smaller than the measured values; the differences are approximately 1.5 eV. In both DFT-linear muffin thin orbital (LMTO) and DFT full potential linear augmented plane wave (FP-LAPW) generalized gradient approximation (GGA) calculations, the band gap values were found around 2.4 eV [74,79]. The empirical pseudo potential band structure calculations for c-GaN have predicted the room temperature band gap values which are 0.3 -0.1 eV less than that of w-GaN [75, 77].

There is a considerable interest to study the properties of zinc-blende BN because it has useful physical properties like extreme hardness, high melting points, interesting dielectric and thermal characteristics. Because it has high resistively ($10^8\Omega$-m), high thermal conductivity (1300W/m-c) and wide band gap (~6eV). Both n- type and p- type of c-BN makes this compound important in the manufacture of electronic devices [89-91].

BN is known to be a very hard material and the only report of its bulk modulus (465±50 GPa) [92] is an inter polar based on empirical relation for the elastic constant for zinc blende structure. This value is larger than the accepted value for diamond (442GPa) [93, 94], but in agreement with the value of 367 GPa [95].

In a recent work, c-BN has been reported to be an ideal substrate for the fabrication of high temperature UV and blue light emitting diodes (LEDs) [89, 96, 97] and laser diodes (LDs) [98]. In the literature, c- BN single crystals have been generally synthesized by a temperature gradient

method under high pressure and high temperature conditions using a proper purified solvent system [99, 100]. On the other hand, c-BN thin films in high quality required for the electronic devices have been grown in a recent work [101] by plasma-enhanced chemical vapor deposition (PECVD) technique.

The wide band gap of c-BN was measured to be approximately 6.2 eV by the optical absorption edge [102], the resonant soft x-ray emission and total photon yield spectra[99], and cathode luminescence spectra measurements, these quantities were measured with experimental side. In the theoretical side, the lattice constant of c-BN has been calculated to be in the range of 3.575-3.649 A by the first principles [103- 110] and molecular dynamics (MD) [109] calculations. In the same theoretical works [103-107, 109], the bulk modulus for BN was measured to be (365 -397GPa). In the literature, the first principles electronic band structure calculations within either local density approximation (LDA) or both LDA and generalized gradient approximation (GGA) or both LDA and Greens functions (GW) approximations have given the indirect band gap of c-BN in the range of 4.19-6.3 eV [103, 104, 107, 110-115].

The last compound of the present work, cubic boron phosphide (c-BP) has also technological importance in the manufacture of electronic devices operating at high temperatures, InP/BP and BP/Si hetero junction bipolar transistors [116]

Because, single crystal BP has high thermal conductivity comparable to that of BN [117]. Furthermore, because of its low reflectivity [118] and it's band gap ~2 eV [119, 120], BP have been utilized as a window layer provided in p-n junction solar cell [121] for transmitting sun light. In the literature, the structural properties of c-BP have been determined by the experimental lattice constant equal 4.54 A [122, 123], bulk modulus of 152-267GPa [122, 124, 125], and the cohesive energy of 10.24eV/atom pair [103] estimated by the experimental heat of formation and heat of atomization energies of B and P. The DFT calculations either by pseudo potential plane wave (PPPW) [103, 104, 126-128] and full potential plane wave (FPPW) [107, 113, 129] or linear muffin thin orbital (LMTO) [126, 130], and linear combination of atomic orbital (LCAO) [126, 130, 131] methods within either LDA and GGA have given the lattice constant of c-BP close to the experimental value. The difference is only 0.29-1.43%.

It was reported that the calculated lattice constant of c-BP is becoming very close to its experimental value when both LDA and GGA's are utilized in total energy minimization calculations [113, 129, 131]. The bulk modulus of c-BP calculated by the first principles methods given above [103, 104, 113, 126-131] are in the narrow range of 160-176GPa. The cohesive energy of c-BP is overestimated 11.45eV/atom pair in DFT calculations [130]. In the literature, the first principles electronic band structure calculations within either LDA or both LDA and GW approximations have given the indirect gap of c-BP along the Δ line $\Gamma_{15}^v \to \Delta_{min}$ [103, 104, 107, 112, 126, 128- 131]. The indirect gap values

reported in these works are all underestimated. The other values calculated 1.252 eV [115], 1.9 eV (113), and 1.1 eV [132] scheme are in better agreement with the present calculations .

The electronic band structures of InN, GaN, BP and BN have been calculated by DFT. The results were discussed in the following sections.

3.2 The results

3. 2.1 InN

The zinc-blende structure of InN is characterized by the lattice constant, a. At the first stage of the work, the equilibrium value of a is determined by calculating total energy of InN by FP-LAPW for a set of volumes and fitting these to the Murnaghan equation [133]. We have adopted the value of 0.95 °A for In and 0.79 °A for N as the muffin-tin radius MT. The electronic configuration of InN is In: Kr ($4d^{10}$ $5s^2$ $5p^1$) and N: He ($2s^2$ $2p^3$). In the calculations, the electrons of In is ($1s^2$ $2s^2$ $2p^6$ $3s^2$ $3p^6$ $3d^{10}$ $4s^2$ $4p^2$ $4d^{10}$) are defined as the core electrons and distinguished from the valence electrons of In in ($5s^2$ $5p^1$).

The present lattice constant of InN 5.056 °A is found to be very close to the lattice constant values of 5.07 A [44]; it is only 0.28% smaller than this value, and it is only 0.77% greater than other results 5.017 [134]. On the other hand the present lattice constant is also close to the lattice constant values of 4.986 °A [135], 4.968 [136], 4.964 [137], 4.98 [55], and 4.97 °A [86] calculated by DFT-GGA. The present lattice constant is

approximately 2.09% greater than the other value of 4.95 °A calculated (LMTO) [98].

At the second stage of the work, the FP-LAPW method within the Frame work of the DFT-GGA has been employed to calculate the band structure of InN. Since, this work is planned to be extended to the bowing parameter calculations of alloys correspond to InN in the near future, we have focused mainly on the energy gaps at high symmetry points. It is found that, the band gap of InN is direct in zinc-blende phase, furthermore, the energy bands is in agreement with the results of previous reports [49]. The present band edge at Γ point is non parabolic as it was reported in these works. Since we are unaware of reports of experimental investigations of the electronic properties of c-InN, we couldn't compare the present band gap values with the experimental results. But, the present band gap at Γ point E_g^Γ is found to be close -0.516 eV with respect to the values -0.48 eV it is only 6.98% smaller than the above magnitude given by ETB [130]. The similar negative and positive direct band gap energies were reported before in the literature.
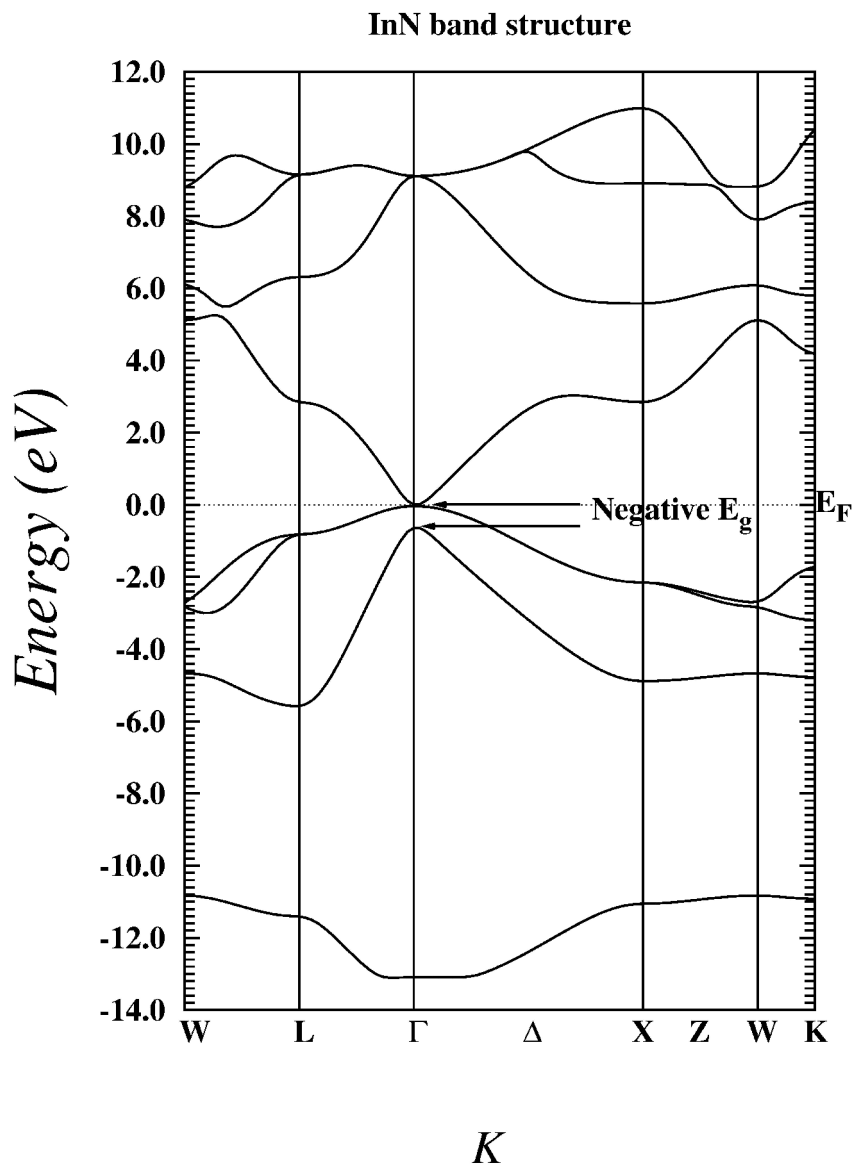
Table (3.1): The theoretical and experimental lattice constant values in °A for InN, GaN, BN, and BP in zinc blende phase.

Compound	theoretical a (°A)	Experimental a (°A)
InN	5.056[A], 4.95[a, b, c] (4.97,5.05)[d], (5.109,4.932)[e] 4.929[f] 4.953[g], 5.004[h], 4.974[i], 5.01[j], 4.983[k], 5.06[l], 5.017[m] 4.92[n], 5.03[o], (4.964, 5.067)[p], 4.968[q]	4.986[r], 4.97[s] 4.98[t]
GaN	4.562[A] 4.433[u], (4.45 ,4.56)[v] (4.518 ,4.59)[h] (4.423, 4.462, 4.45)[w] 4.55[x], 4.5552[y], 4.49[z] 4.461[a"]	4.5[b"], 4.49[c"] 4.530[d"]
BN	3.631[A], 3.591[e"], 3.6006[f"] 3.623[g"], 3.649[h"] 3.626[i"], 3.606[j"] 3.575[k"]	3.615[r"]
BP	4.559[A] 4.558[j"], 4.474[k"] 4.546[j"], 4.551[i"] 4.475[l"] 4.51[m"] 4.554[n"], 4.501[o"]	4.543±0.01[p"] 4.538[q"]

[A] present work, [a] Ref. [84], [b] Ref. [54], [c] Ref. [53], [d] Ref. [85], [e] Ref. [138], [f] Ref. [139], [g] Ref.140 in Ref. [138], [h] Ref. [86], [i] Ref. [141],

[j] Ref. [142], [k] Ref. [143], [l] Ref. [144], [m] Ref. [75], [n] Ref. [145], [o] Ref. [146],

[p] Ref. [147], [q] Ref. [136], [r] Ref. [135], [s] Ref.[44], [t] Ref. [134],

[u] Ref. [84], [v] Ref. [85], [w] Ref. [77], [x] Ref. [78], [y] Ref. [87], [z] Ref. [80], [a"] Ref. [83], [b"] Ref. [68], [c"] Ref. [60], [d"] Ref. [148],

[e"] Ref.[105], [f"] Ref.[106], [g"] Ref. [107, 109], [h"] Ref. [108], [i"] Ref. [113], [j"] Ref. [103], [k"] Ref. [104], [l"] Ref. [127, 128], [m"] Ref. [126, 130], [n"] Ref. [131], [o"] Ref. [129], [p"] Ref. [122], [q"] Ref. [123], [r"] Ref. [149].

In the following step of the present work, the energy parameters of DFT have been derived for c- InN Figure 3.1

InN band structure

$$K$$

Figure (3.1): The energy band structure of c-InN by FP-LAPW

Table (3.2): A summary of the important features, energy gaps and valance bandwidths of the present DFT band structure for c-InN compared to other experimental and theoretical calculation results. All energies are in eV.

	DFT-GGA Our work	LDA-PP	GGA-PP	LDA-FP-LAPW	ETB
$\Gamma_{15}^{V} - \Gamma_{1}^{C}$	-0.517 [a]	(-0.18- -0.40) [b]	-0.55 [c] 0.43 [d]	-0.48 [e] -0.40 [f]	-0.48 [g]

[a] present work, [b] Ref. [47-52], [c] Ref. [49], [d] Ref. [47], [e] Ref. [130],

[f] Ref. [150], [g] Ref. [151]

The band structure of c-InN recalculated by DFT-GGA is shown in Fig. 3.1. The important features of the band structure at high symmetry points are listed in table 3.2. In view of Fig. 3.1. The present direct gap of DFT- GGA (E_g^{Γ}) of c-InN is approximately given a similar value calculated by GGA-PP [49] and ETB [151]

3.2.2 c-GaN

The zinc-blend structure of GaN is characterized by the lattice constant, a. The equilibrium value of a is determined by calculating the total energy of c-GaN using FP-LAPW for a set of volumes and fitting these to the Murnaghan equation [133]. We have adopted the value of 1.164 °A for Ga and 0.79 °A for N as the MT radii. The electronic configuration of GaN is Ga: Ar ($3d^{10} 4s^2 4p^1$) and N : He ($2s^2 2p^3$). In the calculations, the electrons of Ga in ($1s^2 2s^2 2p^6 3s^2 3p^6$) are defined as the core electrons and distinguished from the valence electrons of Ga in ($3d^{10} 4s^2 4p^1$). Similarly, the inner valence electrons of N in ($1s^2 2p^3$) are

distinguished from the valence electrons of N in ($2s^2$ $2p^3$) shell. The equilibrium lattice constant of c-GaN is calculated to be 4.562 °A. The present lattice constant is given in table 3.1 together with the experimental and other calculated lattice constant values of c-GaN presented in the literature. The present value of lattice constant for c-GaN is found to be very close to the result of 4.53 °A [61] measured by X-ray diffraction. The present value of a is only (1.4, 1.6) % greater than other experimental results, 4.5 [68] and 4.49 °A [60], they are measured by X-ray diffraction and optical absorption measurements, respectively. On the other hand, the lattice constant of c-GaN used in the present work is also very close to the values of 4.56 [85], 4.55 [78], 4.552 [87] and 4.59 [86] calculated by pseudo potential with self interaction correction (PP-SIC), DFT/FP-LAPW-GGA with quasi particle correction, DFT/FP-LAPW-LDA, and DFT/PPPW-GGA, respectively. The discrepancy between the present lattice constant and the one 4.518 °A calculated by DFT/PPPW-LDA is only 0.96%. The present lattice constant of c-GaN is greater than the values calculated by FHI96MD, CASTEP, VASP codes [77], zero temperature Green's function formalism [80], non-corrected PP [85], self consistent linear muffin tin orbital (SCLMTO) [84], and FP-APW-local orbital methods [83].

We have employed DFT/FP-LAPW-GGA method in the band structure calculations of c-GaN. It is found that the band gap of GaN is direct in zinc-blend phase, furthermore, the band structure is in close agreement with the PPPW results of previous reports [71]. The present

DFT calculations within GGA do not give any new feature on the band structure of DFT-LDA, only the present (E_g^Γ) 1.494 eV of c-GaN is slightly smaller than the previously reported values of DFT-LDA [72]. This is a widely accepted result that the (DFT-GGA) or (LDA) electronic band structure are qualitatively in good agreement with the experiments in ordering of the energy levels and the shape of the bands, but whose band gap values are always smaller than the experimental data.

The important features of the band structure at high symmetry points are listed in Table 3.3. As it is observed in Fig. 3.2, the valence band structure of c-GaN by DFT-GGA gave the result which was close to direct band gap by DFT - QP [86] and EPP [85, 87], but the present value is only (7.09) % smaller than PP – GB [70].
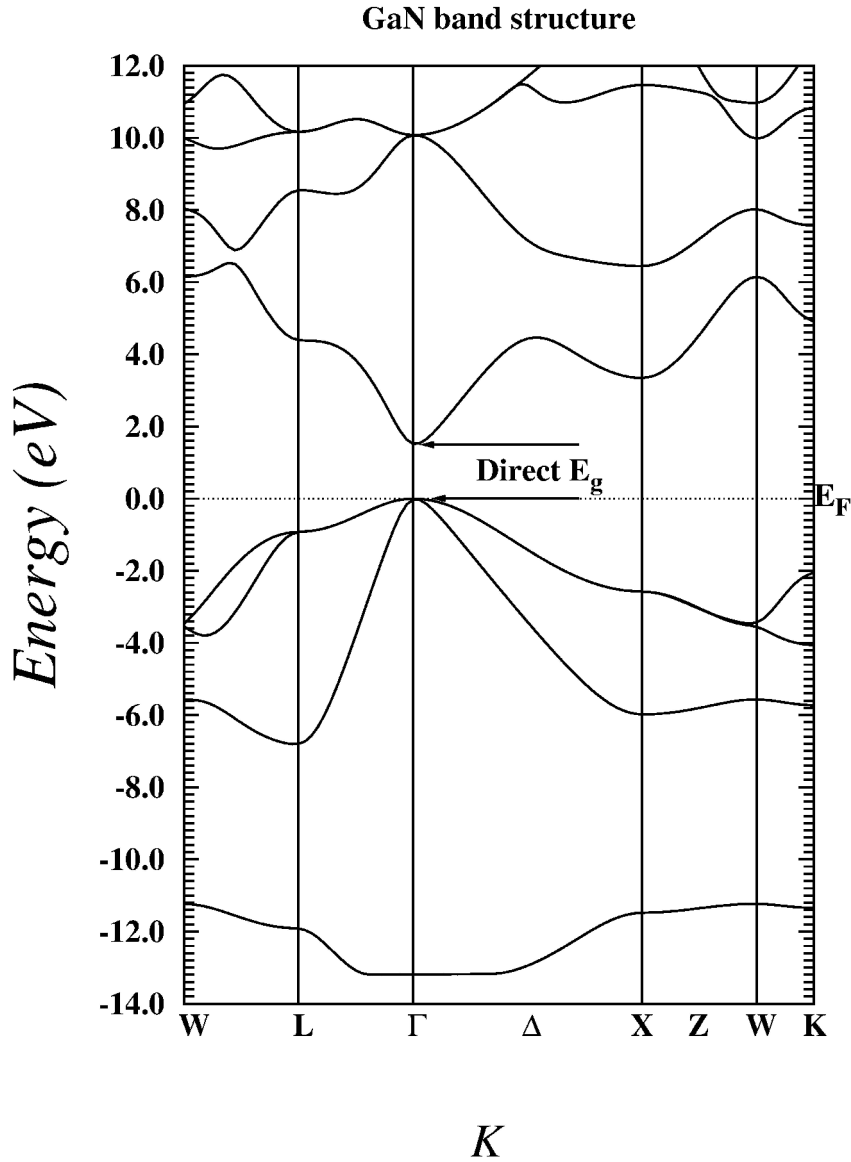
GaN band structure

Figure (3.2): The energy band structure of c-GaN by FP-LAPW by DFT-GGA

Table (3.3): A summary of the important features, energy gaps and valance bandwidths of the present DFT band structure for c-GaN compared to other experimental and theoretical calculation results. All energies are in eV.

	DFT-GGA	DFT-LDA	AE	DFT-QP	PP-GP	PPPW	EPP
$E_g(eV)$ $\Gamma_{15}^{V}-\Gamma_{1}^{C}$	1.494 [a]	1.9 [b] 1.8 [c]	2 [d]	1.6 [e]	1.6 [f]	1.28 [g]	1.6 [h] 1.72 [i]

ª present work, ᵇ Ref. [82], ᶜ Ref. [74], ᵈ Ref. [73], ᵉ Ref. [86], ᶠ Ref. [70], ᵍ Ref.[72], ʰ Ref. [85], ⁱ Ref. [87].

3.2.3 c- BN

The zinc-blende structure of BN is characterized by the lattice constant, a. The equilibrium value of a is determined by calculating the total energy of c-BN using FP-LAPW for a set of volumes and fitting these to the Murnaghan equation [133]. We have adopted the value of 0.85 °A for B and 0.79°A for N as the MT radii. The electronic configuration of BN is B, He :$(2s^2 2p^1)$ and N : He

$(2s^2 2p^3)$. In the calculations, the electrons of B in $(1s^2)$ are defined as the core electrons and distinguished from the valence electrons of B in ($2s^2$ $2p^1$). Similarly, the inner valence band electrons of N in $(1s^2)$ are distinguished from the valence band electrons of N in $(2s^2 2p^3)$ shell. The equilibrium lattice constant of c-BN is calculated to be 3.631°A. The present lattice constant is given in Table 3.1 together with the experimental and other calculated lattice constant values of c-BN presented in the literature. The present value of a is only (1.5 ,0.14)% greater than other results, 3.575 [104] and 3.626°A [113]. On the other hand, the lattice constant used in this work of c-BN is also very close to other values 3.588, 3.631, 3.625, 3.746 A calculated by LDA, PBE-GGA, PW-EV-GGA, and EV-GGA respectively.

We have employed DFT/FP-LAPW-GGA method in the band structure calculations of c-BN. Table. 3.4 gives the important features of the present and previously reported band structures for c-BN at high symmetry points, it is only (3.5) % greater than other value calculated by PWG [152].

Table (3.4) A summary of the important features, energy gaps and valance bandwidths of the present DFT band structure for c-BN compared to other experimental and theoretical calculation results. All energies are in eV.

E_g in eV	DFT-GGA [a]	OPW [b]	PWG [c]	APW [d]
$\Gamma_{15}^{v} - X_{1}^{c}$	4.459	3	4.3	7.2

[a] present calculation, [b] OPW [153] , [c] PWG [152] , , [d] APW [154].

The band structure of c-BN using DFT-GGA is shown in Fig. 3.3. The important features of the band structure at high symmetry points are listed in Table 3.4. As it is observed in Fig. 3.3, the valence band structure of c-BN by DFT-GGA gave approximately the similar result which was obtained using PWG [152], and only the present E_g 4.459 eV of c-BN is slightly greater than the previously reported values of orthogonalized-plane wave OPW [153] and plane-wave-gaussian PWG [152]. But the present fundamental band gap of c-BN is still smaller than the experimental value reported by Augmented plane wave APW [154].

The present DFT calculations within GGA do not give any new feature on the band structure of DFT-LDA. This is an accepted result that the DFT-GGA electronic band structure are qualitatively in good

agreement with the experiments in what concerns the energy levels and the shape of the bands. The energy band structure of c-BN by DFT/FP-LAPW-GGA is shown in Fig 3.3
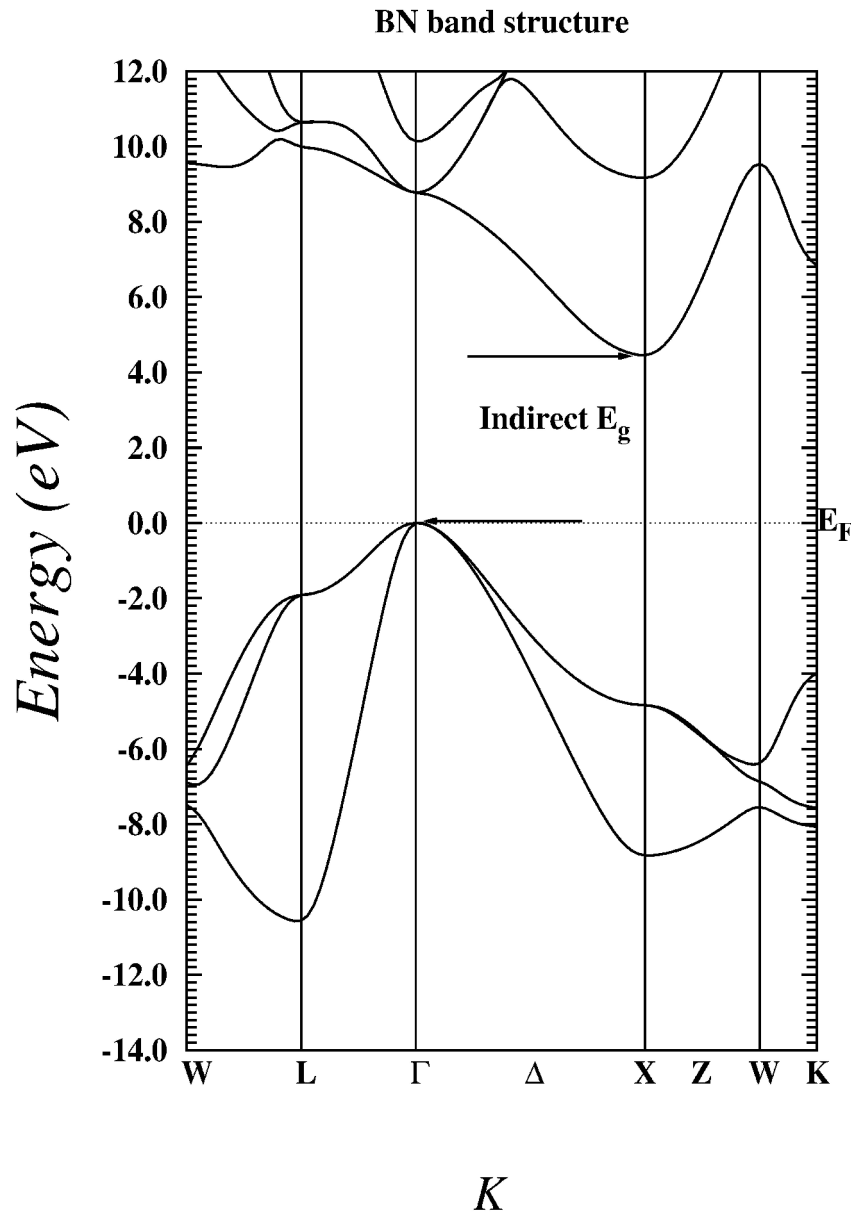
Fig (3.3) band structure of c-BN by DFT/FP-LAPW-GGA

3.2.4 c-BP

The zinc-blende structure of BP is characterized by the lattice constant, a. The equilibrium value of a is determined by calculating the

total energy of c-BP using FP-LAPW for a set of volumes and fitting these to the Murnaghan equation [133]. We have adopted the value of 0.79 °A for B and 0.95 °A for P as the MT radii. The electronic configuration of B: He ($2s^2$ $2p^1$) and P: Ne ($3s^2$ $3p^3$). In the calculations, the electrons of P is ($1s^2$ $2s^2$ $2p^6$) are defined as the core electrons and distinguished from the valence electrons of P in ($3s^2$ $3p^3$). Similarly, the inner shell the experimental and other calculated lattice constant values of BP presented in the literature.

The present lattice constant of BP 4.559 °A is found to be close to other results 4.554 ref. [131] by this calculation; it is only greater than the other theoretical results 4.474°A ref. [104], 4.546°A ref. [103], 4.551°A ref. [113], 4.538 °A ref. [123], 4.475°A ref. [128,127], and 4.51°A ref. [126, 130] as shown in table 3.1.

At the second stage of the work, the FP-LAPW method within the frame work of the DFT has been employed to calculate the band structure of BP. Since, this work is planned to be extended to the bowing parameter calculations of alloys corresponds to BP in the near future, we have focused mainly on the energy gaps at high symmetry points as shown in table 3.5. It is found that, band gap of BP is 1.259 eV in indirect Γ-Δ_{min} in zinc-blend phase, furthermore, this energy bands E_g at Γ- Δ_{min} point (1.259 eV) is (42%) smaller than the theoretical results of previous reports using EPM [155], Semi-ab-initio approach [156], and optical absorption [157] calculated by indirect way.

Table (3.5): A summary of the important features, energy gaps and valance bandwidths of the present DFT band structure for c-BP

Reference	Indirect energy gap eV	
a	1.259	$\Gamma_{15}^{v} - \Delta_{min}$
b	2.2	$\Gamma_{15}^{v} - X_{1}^{c}$
c	2	$\Gamma_{15}^{v} - L_{1}^{c}$
d	2	$\Gamma_{15}^{v} - X_{1}^{c}$

[a] present calculation ,[b] EPM (155) ,[c] semi-ab-initio approach (156) , [d] optical absorption (157).
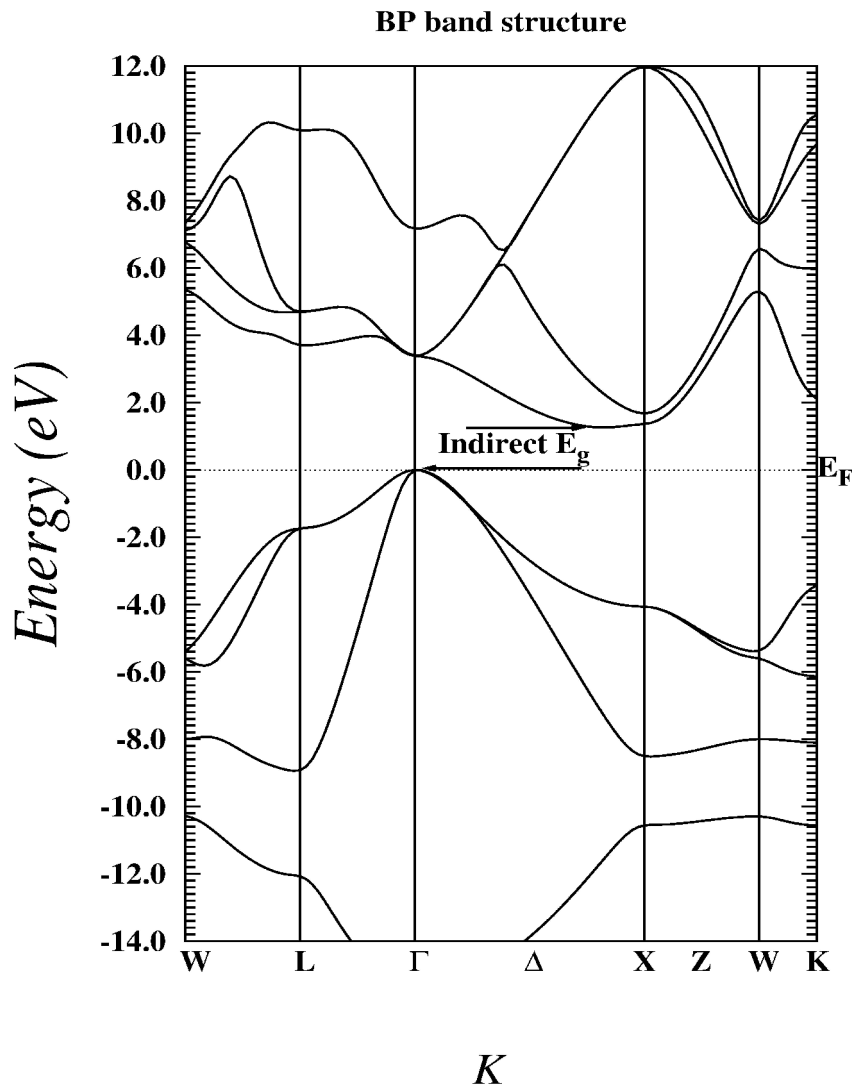
BP band structure

Fig (3.4) : The energy band structure of c-BP by FP-LAPW

CHAPTER FURE
THE ELECTRONIC BAND STRUCTURE OF
BN_xP_{1-x}, $Ga_xB_{1-x}N$, AND $B_xIn_{1-x}N$ ALLOYS

4.1 Introduction

A new class of semiconductor alloys in which one of the constituent elements is replaced by an element with highly dissimilar properties has been discovered recently. These new ternary semiconductor alloys exhibit a range of unexpected characteristics. Particularly, we have aimed to combine c-BN and c-BP compounds, c-BN to c-GaN, and c-BN to InN having different structural and electronic properties in order to obtain new materials BN_xP_{1-x} , Ga_xB_{1-x} N and B_xIn_{1-x} N ternary alloys, with intermediate properties. Therefore these ternary alloys are potential materials for room temperature infrared detectors gas sensors and lasers.

In this work the electronic structure of BN_xP_{1-x}, Ga_xB_{1-x} N and B_xIn_{1-x} N ternary alloys has been calculated using DFT within GGA method. In these calculations, the ternary alloys were defined by only specific concentrations of N ,Ga, In, and B. The calculations have been performed on alloys to introduce the band gaps and lattice constants of the bowing corresponds to the total range of nitrogen, boron, and gallium concentrations(x) with small increments disregarding the so long computational time.

At the first stage of the work, the total energy of each alloy is calculated for diffrent volumes at each concentration. The total energy of

the unitcell at each volume is fitted to Murnaghan equation [133]. The volume with minimum energy is considered as where the equilibrium volume. The Bulk moduli and its derivative are also calculated from Murnaghan equation [133].

After that, the calculated values of the lattice parameters were used to calculate the band structure for the alloys.

The last stage, the energy gap and cohesive energy per/ atom pair were calculated.

The calculated lattice constant and energy gap of the alloys were fitted to the following equations

$$a_{AB_xC_{1-x}} = a_{AB}(x) + a_{AC}(1-x) + b(x)(1-x)$$

$$E_{g_{AB_xC_{1-x}}} = E_{g_{AB}}(x) + E_{g_{AC}}(1-x) + b(x)(1-x)$$

The results of the alloys considered in this work are discussed in the following sections.

4.2 Electronic structure of alloys

4.2.1 BN$_x$P$_{1-x}$

In III-V semiconductors, the replacement of a few percent of the group V element by small, highly electronegative and isoelectronic nitrogen atoms results in a drastic reduction of the fundamental band gap. This effect of N has been confirmed experimentally.

The bowing parameter (b) of the band gap of BN_xP_{1-x} alloy has been performed by FP-LAPW implemented in WIEN2k code [160] . The BN_xP_{1-x} alloys have been modeled with ordered structures of 8atoms/unitcell. The calculation have been done for different composition of nitrogen (x) changing in the total range (0<x<1). The equilibrium lattice constant of the alloys have been obtained by minimizing the total energy with respect to the volume of the unit cell. The lattice constant, bulk modulus, first order pressure derivative of bulk modulus, total energy/cell, cohesive energy/ atom-pair, and band gap of the BN_xP_{1-x} alloys have been calculated using the equilibrium lattice constants and tabulated in table 4.1.

The variation of the lattice constant, and energy gap of the alloys have been plotted as afunction of nitrogen concentration as shown in Figs. (4.1, 4.2) respectively. In the same figures, the variation of the corresponding values calculated by linear concentration dependence rule [161] has been also shown, for comparison.

The equilibrium lattice constants of the BN_xP_{1-x} alloys have been found to be deviated from the corresponding values of the linear concentration rule with a downward bowing parameters of 0.464 A Fig.4.1.

In the present work it is found that, the BN_xP_{1-x} alloys are all direct gap materials. The minimum energy gap between the conduction and valence band of BP is shifted to Γ point from Δ_{min} by addition of nitrogen atoms. Fig. 4.2 shows that, the band gap of BP is decreased more than 1eV by added nitrogen concentration of 0.25. The band gap bowing parameter of the alloys has been calculated to be 9.924eV by fitting the values to a

polynomial function. In the present work, the overall band gap bowing parameter of the BN_xP_{1-x} alloys has been also calculated by the equations of Bernard and Zunger [161] for x = 0.5. Since the compositional effect on the bowing is considered to be small, the band gap bowing equations of Bernard and Zunger have been defined by only the contribution of the volume deformation (b_{VD}), charge transfer(b_{CT}) and the structural relaxation (b_{SR}) of the alloys as follows

$b = b_{VD} + b_{CT} + b_{SR},$

$b_{VD} = 2[E_{BN} (a_{BN}) - E_{BN} (a) + E_{BP} (a_{BP}) - E_{BP}(a)],$

$b_{CT} = 2[E_{BN} (a) + E_{BP}(a) - 2E_{BNP}(a)],$

$b_{SR} = 4[E_{BNP}(a) - E_{BNP}(a_{eq})]$

Here a_{BN}, a_{BP}, and a_{eq}, are the equilibrium lattice constants of BN, BP, $BN_{0.5}P_{0.5}$ alloys, respectively. The lattice constant (a) is calculated by linear composition dependence [161] for the alloys. In the equations, the correspondence lattice constant is used to calculate the energy gap E_g for the compounds and alloys. The band gap bowing parameter of the BN_xP_{1-x} alloys is obtained to be 9.924 eV from the above equations and its equal to 9.921 eV using DFT-GGA ref [162]. Therefore the band gap bowing is mainly originated from the charge transfer in the alloys due to the large electro-negativity deference between N and P atoms. The ignorable contribution of the structural relaxation to the bowing parameter shows the structure model of the atoms which consest the alloys is not necessary. The contribution of the volume deformation due to the mismatching of the

lattice constants of BN and BP is not as big as that of the charge transfer, but it is still important.

Table 4.1 also show the variation of average direct energy gaps as a function of N concentration x in comparison with other energy bands given by PW-EV-GGA method [163] and DFT-GGA method [162]. In view of table 4.1 we note that the overall bowing for Γ point transition is small and downward (direct band gap). Similarly, bowing for X point transition is downward. The present values of E_g^Γ calculated within DFT-GGA are in good agreement with the corresponding values of E_g^Γ calculated within DFT-GGA [162] for BN_xP_{1-x}. For example the present calculated values of E_g^Γ are 0.052eV, 0.388 eV, 1.932 eV and its equal to 0.062eV, 0.376 eV, 1.934 eV within DFT-GGA [162] by persentage error (19%, 3%, and 0.1%) at x= 0.25, 0.50, 0.75 respectively.

Table (4. 1) the minimized energy E_o, the bulk modulus B in GPa, the theoretical lattice constants A a (A), and the energy band gap E_g in eV using zinc blende phase at x=0.25, 0.50 and 0.75 for BN_xP_{1-x}

X	0.25	0.5	0.75
a (A)	4.403 [a], 4.403 [b] 4.4 [c]	3.211 [a], 4.214 [b] 4.21 [c]	3.961 [a], 3.960 [b] 3.96 [c]
B(Gpa)	178.450 [a] 178.47 [b] 182 [c]	213.636 [a] 176.907 [b] 2.09 [c]	264.812 [a] 263.872 [b] 2.61 [c]
B′	3.715 [a] 3.857 [b]	3.380 [a] 2.489 [b]	3.534 [a] 3.914 [b]
E_o (eV)	-2360.995 [a] -2360.996 [b]	-1786.261 [a] -1786.256 [b]	-1211.724 [a] -1211.724 [b]
E_g (eV)	0.052 [a] 0.737 [b] 0.062 [c]	0.088 [a] 1.112 [b] 0.376 [c]	1.932 [a] 2.696 [b] 1.934 [c]
Coh. E/ atom eV	5.316	5.440	5.899

[a] Present work (DFT-GGA), [b] (PW-EV-GGA) ref (163), [c] DFT-GGA[162].
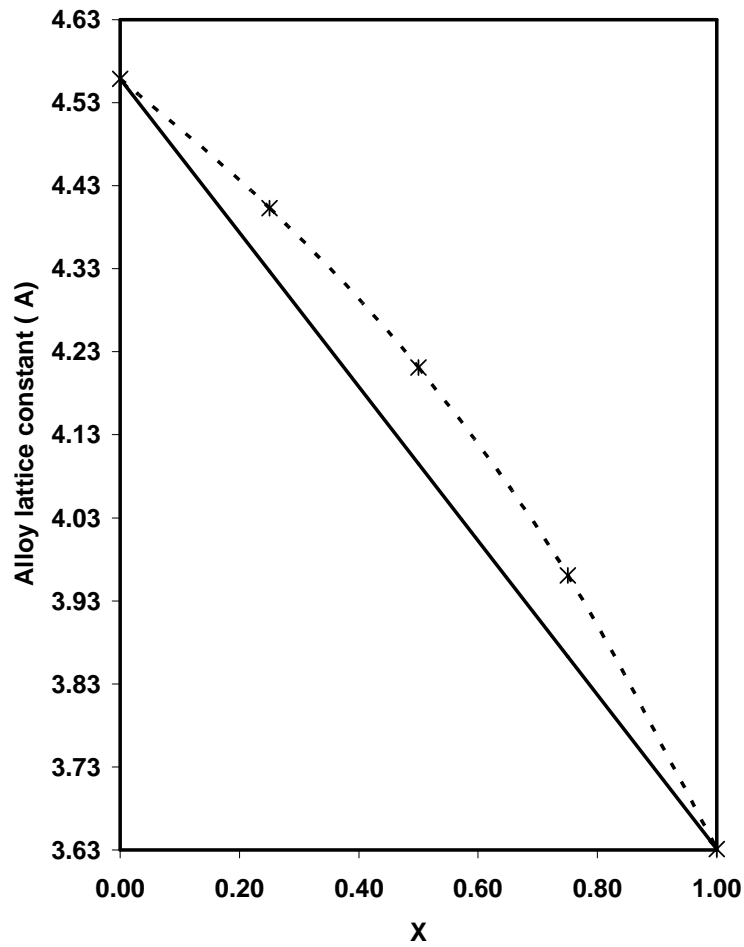
Figure (4.1) Concentration dependence of the lattice constants calculated within DFT-GGA (dotted line) and Vegard's linear rule(solid line) for BN$_{1-x}$P$_X$.
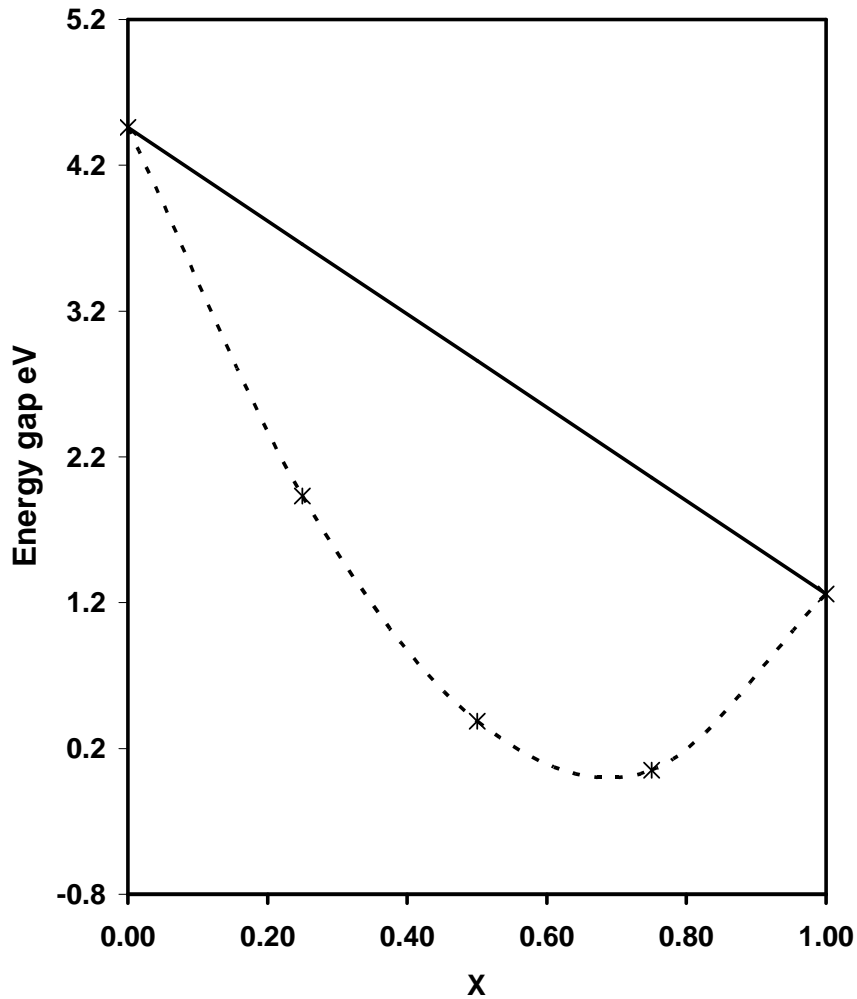
Figure (4.2)   Concentration dependence of the band gap energies calculated within(DFT-GGA) (dotted line) and Vegard's linear rule(solid line) for BN$_{1-x}$P$_X$

4.2.2 Ga$_x$B$_{1-x}$ N

The electronic band structure and lattice constant of Ga$_x$B$_{1-x}$ N alloy with the galium compensating Boron by x= 0.25, 0.5, and 0.75 have been studied in the literature, because of its application in heterostructure system Furthermore, the energy band gap variation of Ga$_x$B$_{1-x}$ N at Γ symmetry point has been also for the full range of the galium concentration theoretically.

The bowing parameter of the band gap and lattice constant of $Ga_xB_{1-x}N$ alloys have been performed by (FP-LAPW) implemented in WIEN2k code [160].

The $Ga_xB_{1-x}N$ alloys have been modeled with ordered structures of 8 atom/unit cell. The calculation have been done for different composition of galium (x) changing in the total range (0<x<1). The equilibrium lattice constant of the alloys have been calculated by minimizing the total energy with respect to the volume of the unit cell. The lattice constant, bulk modulus, first order pressure derivative of bulk modulus, total energy/cell, cohesive energy/ atom-pair, and band gap of the $Ga_xB_{1-x}N$ alloys have been calculated by the equilibrium lattice constants and tabulated in table 4.2. The variation of the lattice constant, and energy gap of the alloys have been plotted with respect to the compositions of galium in Figs.(4.3, 4.4).

The equilibrium lattice constants of the $Ga_xB_{1-x}N$ alloys have been found to be deviated from the corresponding values of the Vegard‚s formula with a downward bowing parameters of 0.399 A Fig. 4.3.

In the present work it is found that, the $Ga_xB_{1-x}N$ alloys are all direct gap materials. The minimum energy gap between the conduction and valence band of BN is shifted by addition of Ga atoms. Fig. 4.4 shows that, the band gap of BN is decreased while added galium concentration of 0.25. The band gap bowing parameter of the alloys has been calculated to be 0.841eV by fitting the values to a polynomial function. In the present work, the overall band gap bowing parameter of the $Ga_xB_{1-x}N$ alloys has been

also calculated by the equations of Bernard and Zunger [161] for x=0.5. Since the compositional effect on the bowing is considered to be small, the band gap bowing equations of Bernard and Zunger have been defined by only the contribution of the volume deformation (b_{VD}), charge transfer (b_{CT}) and the structural relaxation (b_{SR}) of the alloys as follows

$$b = b_{VD} + b_{CT} + b_{SR},$$

$$b_{VD} = 2[E_{GaN} (a_{GaN}) - E_{GaN} (a) + E_{BN} (a_{BN}) - E_{BN}(a)],$$

$$b_{CT} = 2[E_{GaN} (a) + E_{BN}(a) - 2E_{GaBN}(a)],$$

$$b_{SR} = 4[E_{GaBN}(a) - E_{GaBN}(a_{eq})]$$

Here a_{GaN}, a_{BN}, and a_{eq}, are the equilibrium lattice constants of BN, GaN, $Ga_{0.5}B_{0.5}N$ alloys, respectively. The lattice constant (a) is calculated by linear composition dependence [161] for the alloys. In the equations, the correspondence lattice constant is used to calculate the energy gap E_g for the compounds and alloys. The band gap bowing parameter of the $Ga_xB_{1-x}N$ alloys is obtained to be 0.841eV from the above equations. Therefore the band gap bowing is mainly originated from the charge transfer in the alloys due to the large electro- negativity deference between Ga and B atoms. The ignorable contribution of the structural relaxation to the bowing parameter shows the definition of the alloys in the disordered structure model of the atoms is not necessary. The contribution of the volume deformation due to the mismatching of the lattice constants of BN and GaN is not as big as that of the charge transfer, but it is still important.

Table (4.2) the minimized energy, the bulk modulus in GPa, the theoretical lattice constants in A, and the energy band gap in eV for $Ga_xB_{1-x}N$ in zinc blende phase at x=0.25, 0.50, and 0.75 respectively:

X	0.25	0.5	0.75
a. (A)	3.956	4.196	4.386
B (Gpa)	290.524	231.58	197.497
B$'$	4.409	4.302	5.391
E$_o$ (eV)	-4475.596	-8313.986	-12152.558
E$_g$ (eV) $\Gamma_{15}^{v} - \Gamma_{1}^{c}$	3.77	3.334	2.302
Coh. E/atom (eV)	5.643	4.896	4.456
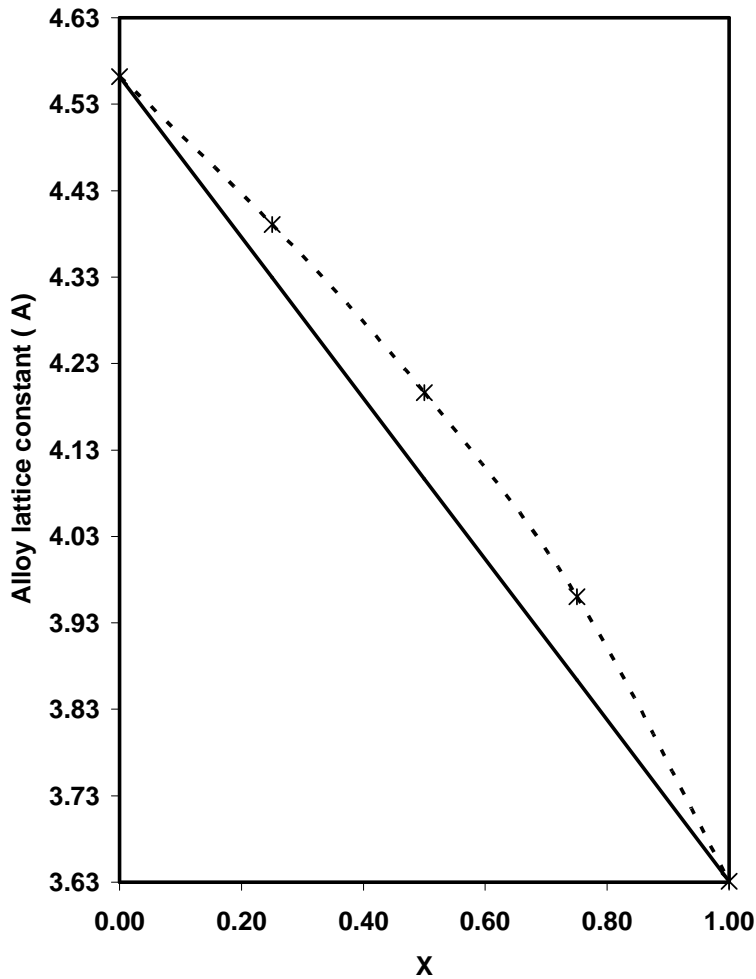
Figure (4.3)   Concentration dependence of the lattice constants calculated within (DFT-GGA) (dotted line) and Vegard's linear rule(solid line) for $Ga_xB_{1-x}N$
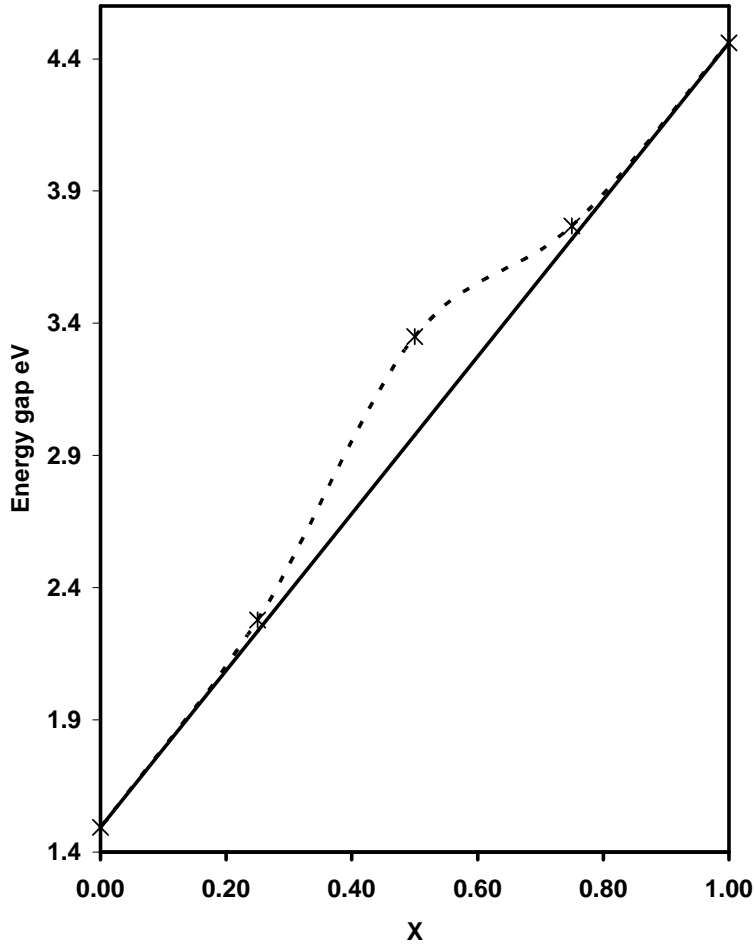
Figure (4.4) Concentration dependence of the band gap energies calculated within (DFT-GGA) (dotted line) and Vegard's linear rule(solid line) for $Ga_xB_{1-x}N$

4.2.3 $B_xIn_{1-x}N$

The electronic band structure and lattice constant of B_xIn_{1-x} Nalloy with the boron concentration of 0.25, 0.5, and 0.75 have been studied in the literature, because of its application in hetero- structure system. Furthermore, the energy band gap variation of $B_xIn_{1-x}N$ at Γ symmetry point has also been for the ubove range of the boron concentration.

The bowing parameter of the band gap and lattice Constant of B_xIn_{1-x} alloys have been performed by (FP-LAPW) implemented in WIEN2k code [160].

The $B_xIn_{1-x}N$ alloys have been modeled with ordered structures of 8 atom/unit cell. The calculation have been done for different composition of boron (x) changing in the total range (0<x<1). The equilibrium lattice constant of the alloys have been calculated by minimizing the total energy with respect to the volume of the unit cell. The lattice constant, bulk modulus, first order pressure derivative of bulk modulus, total energy/cell, cohesive energy/atom-pair, and band gap of the $B_xIn_{1-x}N$ alloys have been calculated by the equilibrium lattice constants and tabulated in table 4.3. The variation of the lattice constant, and energy gap of the alloys have been plotted with respect to the concentration of boron in Figs. (4.5, 4.6).

The equilibrium lattice constants of the $B_xIn_{1-x}N$ alloys have been found to be deviated from the corresponding values of the Vegard's formula with a downward bowing parameters of 0.971 A Fig.4.5.

In the present work it is found that, the $B_xIn_{1-x}N$ alloys are all direct gap materials. The minimum energy gap between the conduction and valence band of BN is shifted by addition of In atoms. Fig. 4.6 shows that, the band gap of InN is decreased while added boron concentration of 0.25. The band gap bowing parameter of the alloys has been calculated to be 0.84eV by fitting the values to a polynomial function. In the present work, the overall band gap bowing parameter of the $B_xIn_{1-x}N$ alloys has been also calculated by the equations of Bernard and Zunger [161] for x=0.5. Since the compositional effect on the bowing is considered to be small, the band gap bowing equations of Bernard and Zunger have been defined by only

the contribution of the volume deformation (b_{VD}), charge transfer (b_{CT}) and the structural relaxation (b_{SR}) of the alloys as follows

$$b = b_{VD} + b_{CT} + b_{SR},$$

$$b_{VD} = 2[E_{BN}(a_{BN}) - E_{BN}(a) + E_{InN}(a_{InN}) - E_{InN}(a)],$$

$$b_{CT} = 2[E_{BN}(a) + E_{InN}(a) - 2E_{BInN}(a)],$$

$$b_{SR} = 4[E_{BInN}(a) - E_{BInN}(a_{eq})]$$

Here a_{InN}, a_{BN}, and a_{eq}, are the equilibrium lattice constants of InN , BN, $B_{0.5}In_{0.5}N$ alloys, respectively. The lattice constant (a) is calculated by Vegard's rule [161] for the alloys. In the equations, the correspondence lattice constant is used to calculate the energy gap E_g for the compounds and alloys. The band gap bowing parameter of the $B_xIn_{1-x}N$ alloys is obtained to be 3.724eV from the above equations. Therefore the band gap bowing is mainly originated from the charge transfer in the alloys due to the large electro-negativity deference between In and B atoms. The ignorable contribution of the structural relaxation to the bowing parameter shows the definition of the alloys in the disordered structure model of the atoms is not necessary. The contribution of the volume deformation due to the mismatching of the lattice constant of BN and InN is not as big as that of the charge transfer, but it is still important.

Table (4. 3): The minimized energy E_o **in (eV), the bulk modulus B in (Gpa), the theoretical lattice constants in A, and the energy band gap** E_g **in (eV) for** $B_x In_{1-x}$ **N in zinc blende phase at x=0.25, 0.50, and 0.75 respectively.**

X	0.25	0.5	0.75
a.(A)	4.213	4.585	4.8395
B(Gpa)	173.169	189.6385	173.169
B′	5	1.5675	5.0
E_o **(eV)**	-35787.029	-24700.034	-35787.029
E_g **(eV)** $\Gamma_{15}^{v} - \Gamma_{1}^{c}$	3.316	0.772	0.001
Coh. E/atom (eV)	4.572	3.621	3.223
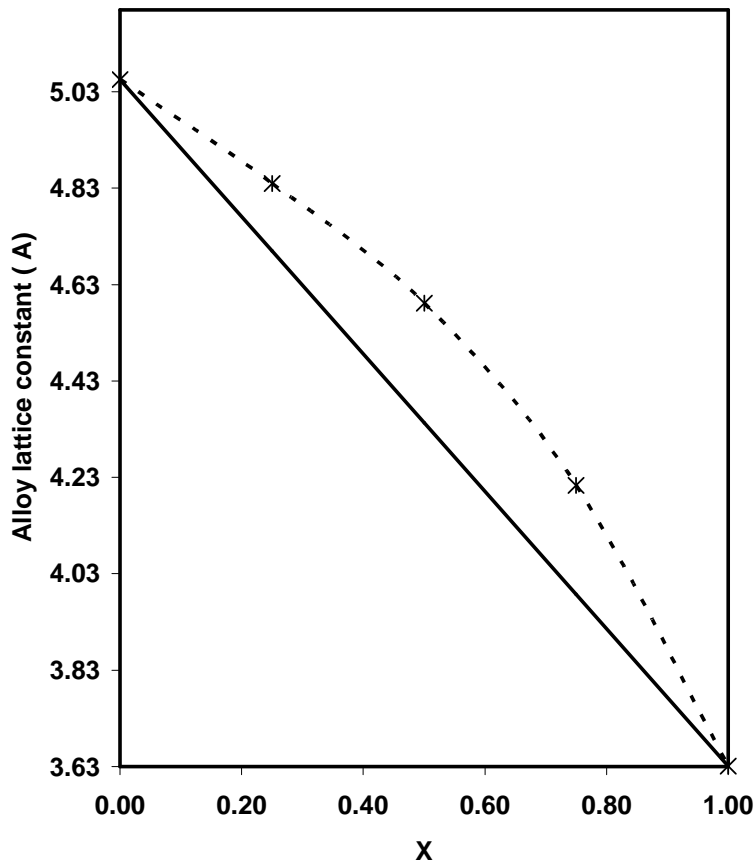
Figure (4.5) Concentration dependence of the lattice constants calculated within (DFT-GGA) (dotted line) and Vegard's linear rule for $B_x In_{1-x} N$

In$_{0.25}$B$_{0.75}$N band structure

Figure (4.6): The energy band structure of B$_{0.25}$In$_{0.75}$N by FP-LAPW

Figure (4.7) Concentration dependence of the band gap energies calculated within (DFT-GGA) (dotted line) and Vegard's linear rule for $B_x In_{1-x} N$
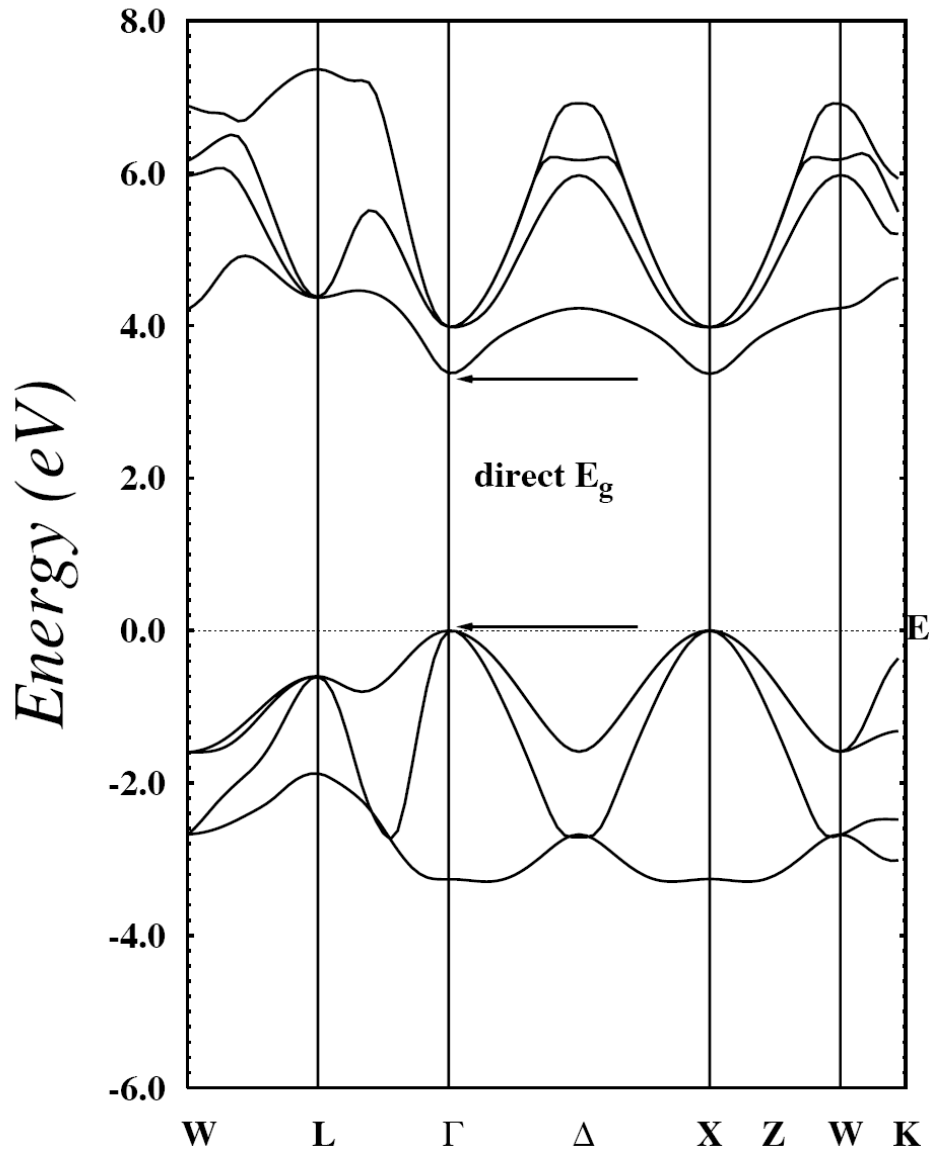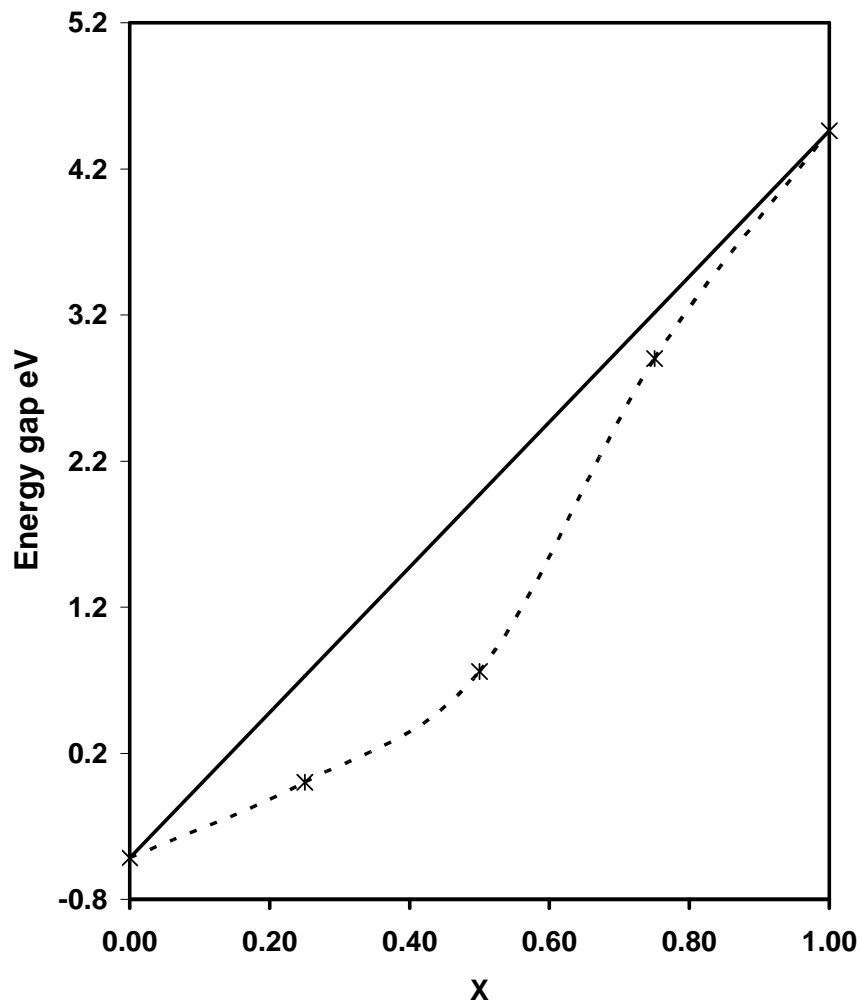
CHAPTER FIVE

CONCLUSIONS

In the present work, FP-LAPW method has been employed to study the structural and electronic properties of BN, BP, InN, and GaNcompounds and their ternary alloys. The equilibrium lattice constant, bulk modulus, first-order pressure derivatives of the bulk moduli and the energy gaps of the compounds at different momentum points have been calculated by generalized gradient approximation of density functional theory DFT- GGA.

The III-V compounds have been considered in zinc-blend phase defined by their equilibrium lattice constants obtained from the present calculations of total energy minimization. The lattice constants of InN, BN, BP and GaN compounds have been calculated within a small discrepancy compared to the experimental average values for BN BP, GaN and InN as discussed before in chapter three. The present DFT-GGA calculations have shown direct band gap structures in zinc-blend phase for InN and GaN, and indirect band gap for BP and BN. However the conduction band minima of all the above compounds located at Γ- Γ symmetry point, Γ- Δ_{min}, and Γ- X respectively . The energy gaps by the present DFT-GGA calculations for the above cited compounds at high symmetry points is a widely accepted result in the literature for GaN with DFT-quasi particle (QP) Ref. [86] and non local EPM calculations is accepted to the present calculation for BN. Due to the lack of experimental

results, the calculated direct band gap value of InN has been attempted to improve considering the gap value supplied by corrected DFT-GGA calculations given in the literature.

An important part of this work consists of GGA-DFT calculations in which we have been calculated the structural and electronic band of BN_xP_{1-x}, Ga_xB_{1-x} N and B_xIn_{1-x} N ternary alloys. The variation of the lattice constant, bulk modulus, and the minimum energy band gap of the BN_xP_{1-x}, Ga_xB_{1-x} N, and B_xIn_{1-x} N alloys have been analyzed as a function of the nitrogen, gallium, and boron concentrations respectively in the total range with small increments. The large bowing parameter of the lattice constant of the alloys calculated in this work is due to the large matching between the lattice constant of BN and BP compounds for BN_xP_{1-x}, BN and GaN compounds for Ga_xB_{1-x} N , and BN with InN for B_xIn_{1-x} N. Similarly, the large mismatching of both bulk modules and indirect band gaps BN with BP, or InN, and or GaN causes a large bowing parameter for the bulk modules and the band gap engineering of the alloys. On the other hand, the large bowing parameters calculated in this work showed the invalidity of Vegard's linear rule in the definition of lattice constant, bulk modulus, and minimum energy gap of the BN_xP_{1-x}, Ga_xB_{1-x} N and B_xIn_{1-x} N ternary alloys. In the present work, the effect of the charge transfer on the large band gap engineering of the considered alloys is found to be dominant in the Bernard and Zunger's formalism. The DFT energy parameters of BP, BN, InN, and GaN obtained from the present calculations have been tested by recalculating the energy band structure of the compounds. The band gap

and the valence bandwidth values of c-InN by DFT are found to be very small comparing with the other values given in table 3.2 .

The good agreement between the present and average equilibrium lattice constant values of c-InN might have acontribution to obtain good band gap energies. In the present DFT calculations, the direct band gap of GaN is found to be less than the value of the band gap calculated by the same approximation. A small discrepancy is also found between the present and reported valence band width values of BP. But DFT calculations of InN of the direct band gap is (-0.516 eV) [with respect to the smallest discrepancy (0.033 eV) (0.0.036 eV) belongs to a theoretical result reported before by GGA- PP [49], ETB [151], and EPP as shown in table3.2. The DFT energy parameters of GaN and BN calculations have been also tested by recalculating the energy band structure of the compounds. Since the present DFT equations are formulated only at Γ points , then the first optical transition of the ternary and quaternary alloys of the semiconductor compounds was generally defined at either Γ point. Since the present DFT energy parameters successfully reproduce the band structures of the compounds at Γ - Γ symmetry points, they are considered reliable for the band gap bowing calculations of the BN_xP_{1-x} ,Ga_xB_{1-x} N , and B_xIn_{1-x} N. The calculated fundamental band gap values of BN_xP_{1-x} ternary alloys for different concentration of N, have been studied and compared with other approximations as shown in chapter four. According to the knowledge of authors, this is the first study that calculates the band

structure of bulk B_xIn_{1-x} N and Ga_xB_{1-x} N alloy for complete range of contents.

In the present work, the band structure of BN_xP_{1-x} , $Ga_xB_{1-x}N$, and $B_xIn_{1-x}N$. have been calculated and the variation of E_g^Γ has been investigated with respect to the N, Ga , and In concentration x. The present bowing for Γ point transitions is found to be downward for all BN_xP_{1-x} , $Ga_xB_{1-x}N$, and $B_xIn_{1-x}N$. alloys. But, the numerical value of the bowing parameter for E_g^Γ alloys is not constant in the literature. The difference between the calculated bowing parameters of E_g^Γ for the same alloys might be originated from both different energy gaps and lattice constant values of the compounds.

References

[1] S. N. Mohammad and H. Moorcock, Prog. *Quantum Electronic* **20** (1996) 361.

[2] A. Yamamoto, M. tsujino, M. Ohkubo and A. Hashimoto, Sol. *Energy mater.Sol. Cells*. **35** (1994) 53.

[3] S. Nakamura and G. Fasol, **The blue laser diodes** (Springer,Berlin (1997).

[4] A. Dagar, J. Christen, T. Riemann,S. Richler, J. Blassing, A. Diez, A. Krost, A. Alam and M. Heuken*, Appl.Phys.lett*. **78** (2001) 2211.

[5] I. Vurgaftman, J. R. Meyer, and L. Ram-Mohan, J. *Appl. Phys*. **89** (2001) 5815. and references sited theirin.

[6] **Wide band gap semiconductors**, proceeding of the seventh Trieste Semicon- ductors symposium, 1992, edited by C. G. Van de Walle (North Holland, Amsterdam 1993).

[7] J. F. Kaeding, Y. Wu, T. Fujii, R. Sharma, P. T. Fini, J. S. Speck, and S. Nakamura, J. *Crystal Growth*. **272** (2004) 257.

[8] T. Kawashima, A. Miyazaki, H. Kasugai, S. Mishima, A. Honshio, Y. Miyake, M. Iwaya, S. Kamiyama, H. Amano, and I. Akasaki, J. *Crystal Growth*. **272** (2004) 270.

[9] O. Aktas, Z. F. fan, S. N. Mohammad, A. E. Botchkarev, H. Morkoc, *Appl. Phys. Lett*. **69** (1996) 3872.

[10] K. Wang, R. R. Recber, *Appl. Phys. Lett*. **79** (2001) 1602.

[11] H. C. Casey and M. B. Panish, **Heterostructure lasers** (Academic, New York, (1978), and references therein.

[12] C. E. Volin, J. P. Garcia, E. L. Dereniak, M. K. Descour, T. Hamilton, and R. McMillan, *Appl. Opt***. 40** (2001) 4501.

[13] B. J. Kirby and R. K. Hanson, *Appl. Opt*. **41** (2002) 1190.

[14] M. Osi´ nski, *opto-electro. Rev*. **11** (2003) 321.

[15] T. Aschley, T. M. Burhe, G. J. Pryce, A. R. Adams, A. Andreev, B. N. Murdin, E. P. O'Reilly, and C. R. Pidgeon, *Sol. State Elec*. **47** (2003) 387.

[16] G. B. Stringfellow and P. E. Greene, J**.** *Electrochem. Soc*. **118** (1971) 805.

[17] M. Y. Yen, B. F. Levine, C. G. Bethea, K. K. Choi, and A. Y. Cho, *Appl. Phys. Lett.* **50** (1987) 927.

[18] M. Y. Yen, R. People, K. W. Wecht, and A. Y. Cho, *Appl. Phys. Lett.* **52** (1988) 489.

[19] Z. M. Fang, K. Y. Ma, D. H. Jaw, R. M. Cohen, and G. B. Stringfellow, J. *Appl. Phys*. **67** (1990) 7034.

[20] S. Elies, A. Krier, I. R. Cleverley, and K. Singer, *J. Phys. D* **26** (1993) 159.

[21] K. T. Huang, C. T. Chiu, R. M. Cohen, and G. B. Stringfellow, J. *Appl*. *Phys.* **75** (1994) 2857.

[22] V. K. Dixit, B. Bansal, V. Venkataraman and H. L. Bhat, *Appl. Phys. Lett.* **81** (2002) 1630.

[24] S. Yamaguchi, M. Kariya, S. Nitta, T. Takeuchi, C. Wetzel, H. Amano, and I Akasaki, *Appl. Phys. Lett*. **76** (2000) 876.

[25] S. Yamaguchi, Y. Iwamura, and A. Yamamoto, *Appl. Phys. Lett*. **82** (2003) 2065.

[26] S. Sinharoy, M. A. Stan, A. M. Pal, V. G. Weizer, M. A. Smith, D. M. Wilt, and K. Reinhardt, J. *Crystal Growth*. **221** (2000) 683.

[27] E. A. Pease, L. R. Dawson, L. G. Vaughn, P. Rotella, and L. F. Lester, J. *Appl. Phys*. **93** (2003) 3177.

[28] P. Hohenberg and W. Kohn, *Phys. Rev*. B**864** (1964) 136.

[29] W. Kohn and L. J. Sham, **Phys. Rev. 140** (1965) Al 133.

[30] J. P. Perdew and Y. Wang, *Phys. Rev*. B **45** (1992) 13244.

[31] Hartree, D. R. (1927) *Proc. Campridge Phil. Soc*. **25**, 225, 310.

[32] M. Cardona, J. *Phys. Chem. Solids*, **24** (1963) 1543.

[33] M. Cardona, J. *Phys. Chem. Solids*, **26** (1965) 1351.

[34] W. A. Harrison, *Phys. Today*, **22, 23** (1969) .

[35] J. C. Slater and G. F. Koster*, Phys. Rev*. **94** (1954) 1498.

[36] W. A. Harrison, **Elementary Electronic structure** (World scientific Publish-ing 1999).

[37] Hartree, D. R. (1927) Proc. Campridge Phil. Soc. 25, 225, 310.

[38] V. Fock, *Z. Phys*. **61** (1930) 126.

[39] P. Hohenberg and W. Kohn*, **Phys. Rev.** B***864** (1964) 136.

[40] W. Kohn and L. J. Sham, *Phys. Rev*. **140** (1965) Al 133.

[41] J. Wu, W. Walukiewicz, K. M. Yu, J. W. Ager III, E. E. Haller, H. Lu, W. J. Schaff, Y. Saito, and Y. Nanishi*, **Appl .Phys Lett**. **80** (2002) 3967.

[42] T. Matsuka, H. Ohamoto, M. Nakao, H. Harima, and E. Kurimoto, ***Appl. Phys. Lett***. **81** (2002) 1246.

[43] A. Tabata, A. P. Lima, L. K. Teles, L. M. R. Scolfaro, J. R. Leite, V. Lemos, B. Sch¨ottker, T. Frey, D. Schikora, and K. Lischka, *Appl. Phys. Lett*. **74,** (1999) 362 **.** A. P. Lima, A. Tabata, J. R. Leite, S. Kaiser, D. Schikora, B.Sch¨ottker, T. Frey, D. J. As, and K. Lischka, J. *Crystal Growth* **202** (1999) 396.

[44] C. Stampfl and C. G. Van de Walle, *Phys. Rev*. B **59** (1999) 5521.

[45] V. Lemos, E. Silveira, J. R. Leite, A. Tabata, R. Trentin, L. M. R. Scolfaro, T. Frey, D. J. As, D. Schikora, and K. Lischka, *Phys. Rev. Lett.* **84** (2000) 3666.

[46] V. Cimalla, J. Pezoldt, G. Ecke, R. Kosiba, O. Ambacher, L. Spieb, G. Teichert, H. Lu, And W. J. Schaff**,** *Appl. Phys. Lett*. **83** (2003) 3468.

[47] F. Bechstedt and J. Furthmüller, J**.** *Cryst. Growth* **246**, 315 (2002).

[48] M. Fuchs, J. L. F. Da Silva, C. Stampfi, J. Neugebauer, and M. Scheffler**,** *Phys. Rev*. B **65**, (2002) 245212.

[49] 13 C. Stampfl and C. G. Van de. Walle**,** *Phys. Rev*. B **59**, (1998) 5521.

[50] 14 M. St edele, J. A. Majewski, P. Vogl, and A. G rling, *Phys. Rev. Lett.* **79**, (1997) 2089. (World Scientific, London, 2002), 222–232.

[51] 15 D. Vogel, P. Krüger, and J. Pollmann, *Phys. Rev***.** B **55**, (1997) 12836.

[52] 19 N. E. Christensen and I. Gorczyca, *Phys. Rev*. B **50**, (1994) 4397.

[53] F. Bechstedt, and J. Furthm¨ uler, J**.** ***Crystal Growth*** **246** (2002) 315.

[54] D. Bagayoko, L. Franklin, and G. L. Zhao, J. *Appl. Phys*. **96** (2004) 4297.

[55] D. Chandrasekhar, D. J. Smith, S. Strite, M. Lin, and H. Morko¸ c, J. *Crystal Growth* **152** (1995)135.

[56] Y.-F. Wu, B. P. Keller, S. Keller, D. Kapolnek, P. Kozodoy, S. P. Denbaars, and U. K. Mishra, *Appl. Phys. Lett*. **69** (1996) 1438.

[57] S. Nakamura, J. *Crystal Growth*, **202** (1999) 290.

[58] G. Ramirez-Flores, H. Navarro-Contreras, A. Lastras-Martinez, R. C. Powell, and J. E. Greene, *Phys. Rev*. B **50** (1994) 8433.

[59] T. Lei, T. D. Moustakas, R. J. Graham, Y. He, S. J. Berkowitz, J. *Appl. Phys*. **71** (1992) 4933.

[60] R. C. Powell, N.-E. Lee, Y.-W. Kim, and J. E. Greene, J. **Appl. Phys**. **73** (1993) 189.

[61] Physics of Group IV Elements and III-V Compounds of Landolt-Bornstein, numerical data and Functional Relationships in Science and Technology: New series, Group III, Vol. 17. a, edited by O. Modelung, M. Schultz and H. Weiss (Springer, Newyork, (1982). [62] J. Menniger, U. Jahn, O. Brandt, H. Yang, and K. Ploog, *Phys. Rev*. B**53** (1996) 1881.

[63] D. J. As, F. Schmilgus, C. Wang, B. Sch¨ ottker, D. Schikora, and K. Lischka, *Appl. Phys. Lett*. **70** (1997) 1311.

[64] H. Okumura, H. Hamaguchi, T. Koizumi, K. Balakrishnan, Y. Ishida, M. Arita, S. Chichibu, H. Nakanish, T. Nagatomo, S. Yoshida, J. *Crystal Growth*, **189** (1998) 390.

[65]   C. Adelmann, E. Martinez Guerrero, F. Chabuel, J. Simon, B. Bataillou, G. Mula, Le Si Dang, N. T. Pelekanos, B. Daudin, G. Feuillet and H. Mariette*, Mat. Sci. and Eng*. B **82** (2001) 212

[66] D. Xu, H. Yang, J. B. Li, D. G. Zhao, S. F. Li, S. M. Zhuang, R. H. Wu, Y. Chen, and G. H. Li*, Appl. Phys. Lett*. **76** (2000) 3025.

[67] S. Strite, J. Ran, Z. Li, A. Salvador, H. Chen, D. J. Smith, W. J. Choyke, and H. Morkoc, J. *Vac. Sci. Technol*. B **9** (1991) 1924.

[68] Z. H. Feng, H. Yang, X. H. Zheng, Y. Fu, Y. P. Sun, X. M. Shen, and Y.T. Wang, *Appl. Phys. Lett***. 82** (2003) 206.

[69] J. Petalas, S. Logothetidis, S. Boultadakis, M. Alouani, and J. M. Wills, *Phys. Rev*. B **52** (1995) 8082.

[70] D. Vogel, P. Krueger, and J. Pollmann, *Phys. Rev*. B **55**, (1997) 12 836.

 [71] A. F. Wright and J. S. Nelson, *Phys. Rev*. B **5**1, (1995) 7866. [72] C. Stampfl and C. G. Van de Walle Xerox Palo Alto Research Center, 3333 Coyote Hill Road, Palo Alto, California **59** (1998) 94304.

[73] V. Fiorentini, M. Methfessel, and M. Scheffler, *Phys. Rev.* B **47**, (1993) 13 353. J. A. Thornton, and J. E. Greene, in Diamond, Silicon Carbide.

[74] G. Ramirez-Flores, H. Navarro-Contreras, A. Lastras-Martinez, R. C. Pow-ell, and J. E. Greene, *Phys. Rev*. B **50**, (1994) 8433.

[75] W. J. Fan, M. F. Li, T. C. Chong, and J. B. Xia, J. *Appl. Phys.* **79** (1996)188.

[76] A. Tadjer, B. Abbar, M. Rezki, H. Aourag, and M. Certier, J. *Phys. Chem. Solids* **60** (1999) 419.

[77] S. K. Pugh, D. J. Dugdale, S. Brand, and R. A. Abram, *Semicond. Sci. Technol.* **14** (1999) 23.

[78] V. I. Gavrilenko and R. Q. Wu, *Phys. Rev*. B **61** (2000) 2632.

[79] C. Persson, A. Ferreira da Silva, R. Ahuja, and B. Johansson, J. *Crystal Growth*, **231** (2001) 397.

[80] C. Persson, Bo E. Sernelius, R. Ahuja, and B. Johansson, J*. Appl. Phys.* **92** (2002) 3207.

[81] D. Fritsch, H. Schmidt, and M. Grundmann, *Phys. Rev*. B **67** (2003) 235205.

[82] B. Bouhafs, F. Litimein, Z. Dridi1, and P. Ruterana, *Phys. Stat. Sol.* (b)**236** (2003) 61.

[83] M. B. Kanouna, A. E. Merada, J. Cibert, H. Aourag, G. Merada, *J. Alloys and Compounds*, **366** (2004) 86.

[84] K. Kim, W. R. L. Lambrecht, and B. Segall, *Phys. Rev*. B **53**, (1996) 16 310.

[85] D. Vogel, P. Krger, and J. Pollmann, *Phys. Rev*. B **55**(1997) 12836.

[86] G. Kaczmarczyk, A. Kaschner, S. Reich, A. Hoffmann, C. Thomasen, D.J. As, A. P. Lima, D. Schikora, K. Lischka, R. Averbeck, and H. Riechert, *Appl. Phys. Lett.* **76** (2000) 2122.

[87] L. E. Ramos, L. K. Teles, L. M. R. Scolfaro, J. L. P. Castineira, A. L. Rosa, and J. R. Leite, *Phys. Rev*. B **63** (2001) 165210.

[88] A. Rubio, J. L. Corkill, M. Cohen, E. Shirley, and S. G. Louie, *Phys. Rev*. B **48** (1993) 11810.

[89] O. Mishima, K. Era, J. Tanaka, and S. Yamaoka, *Appl. Phys. Lett*. **53** (1988) 962.

[90] T. Ikeda, Y. Kawate, and Y. Hirai*, J.Vac. Technol*. A**8** (1990) 3168.

[91] S. M. Chore, G. N. Chaudhari, S.V. Manorama, and A.Bath, *Semicond. Sci. Technol*. **17** (2002) 1141.

[92] J. A. Sanjurjo, E. Lopez- Cruz, P. Vogl, and M. Cardona, *Phys. Rev. B* **28**, (1983) 4579.

[93] J. R. Chelikowsky and S. G. Louie, *Phys, Rev*. B **29**, (1984) 3470.

[94] H. G. McSkimin and P. Andreatch, Jr. , J. *Appl. Phys*. **43** (1982) 985.

[95] M. L. Cohen. Phys. Rev. B **32** (1985) 7988.

[96] T. Taniguchi, K. Watanabe, S.Koizumi, I.Sakaguchi, T. Sekiguchi and S. Yamaoka, *Appl. Phys. Lett*. **81** (2002) 41445.

[97] Q-Ping Dou, H-Tao Ma, G. Jia, Z-Guo Chen, K. Cau , C. Ren, J-Xun Zhao, X-Huan Liu, Yu-Hong Zhang, B. Shi, and T-Chen Zhang, *Appl. Phys. Lett.* **88** (2006) 154102.

[98] G. A. Slack, J.*Phys. Chem.* **34** (1973) 321.

[99] A. Agui, S. Shin, M. Fujisawa, Y. Tezuka, T. Ishii, Y. Muramatsu, O. Mishima,and K. Era, *Phys. Rev*. B**55** (1997) 2073.

[100] K. Watanabe, T. Taniguchi, and H. Kanda, *Phys. Stat. Sol*. (a), **201** (2004) 2561.

[101] W. J. Zhang, I. Bello, Y.Lifshiftz, K. M.Chan, Y.Wu, C.Y.

[102] A. Onodera, M. Nakatani, M. Kobayashi, Y. Nisida, *Phys. Rev*. B **48** (1993) 2777.

[103]] R. M. Wentzcovitch, R. J. Chang, and M. L. Cohen, *Phys. Rev*. B **34** (1986) 1071.

[104] P. Rodriguez-Hernandez, M. Gonzalez-Diaz, and A. Munoz, *Phys. Rev*. B **51** (1995) 14705.

[105] K. Karch and F.Bechstedh, *Phys. Rev*. B **56** (1997) 7404.

[106] A. F. Goncharov, J. C. Crowhurst, J. K. Dewhurst, S. Sharma, C. Sanloup, E. Gregoryanz, N. Guignot, and M. Mezouar, *Phys. Rev*. B **75** (2007) 22414.

[107] A. Zaoui and F. El-Haj Hassan, J. *Phys. ; Condens. Matter* **13** (2001) 253.

[108] P. E. Van Camp, V. E. Van Doren, and J. T. Devreese, *Phys. Stat. Sol.* (b) **146** (1988) 573.

[109] W. Sekkal, B. Bouhafs, H. Aourag and M. Certier, J. *Phys.; Condens. Matter*. **10** (1998) 4975.

[110] Y- Nian Xu and W. Y. Ching, *Phys. Rev*. B**44** (1991) 7787.

[111] H. Bross and R. Bader, *Phys. Stat. Sol*. (b) **191** (1995) 369.

[112] K. T. Park, K. Terakura, and N. Hamada, *J. of Phys. C* **20** (1987) 1241.

[113] M. P. Surh, S. G. Louie, and M. L. Cohen, *Phys. Rev B* **43**, 9126 (1991) .

[114] Y. Al-Douri, Solid State Commun. **132** (2004) 465. H. Xia and A. L. Ruoff, J**.** *Appl. Phys.* **74** (1993) 1660.

[115] A. Zaoui and F. El- Haj Hassan, J. *Phys.: Condens. Matter* , 253(2001).

[116] T. Takenaka, M. Takigawa, and K. Shohno, J**.** *Electrochem. Soc.* **125** (1978) 633.

[117] Y.Kumashiro, The Rigaku J. **7** (1990) 21.

[118] M. Takigawa, J. Satoh, K. Shohno, J. *Electrochem. Soc*. **122** (1975) 824.P. Kocinski and M. Zbroszczyk, *Semicond. Science and Technol*. **10** (1995)1452.

[119] R. J. Archer, R. Y. Koyama, E. E. Loebner, andR. C. Lucas, *Phys. Rev. Lett.* **12** (1964) 538.

[120] V.A.Fomichev and M. A. Rumsh, J. *Phys. Chem. Solids* **29** (1968) 1015; V. A. Fomichev, I.I. Zhukova, and I. K. Polushina, J. *Phys. Chem. Solids* **29** (1968) 1025.

[121] A. Goossens and J. Schoonman, *Electrochim. Acta* **40** (1995) 1339.

[122] W.R.L. Lambrecht and B. Segall, *Phys. Rev*. B **43** (1991) 7070.

[123] G. A. Slack and S. F. Bartram, J. *Appl. Phys*. **46** (1975) 89.

[124] W. Wettling and J. Windscheif, *Solid State Commun*. **50** (1983) 33.

[125] T. Suzuki, T. Yagi, and S. Akimoto, J. *Appl. Phys*. **54** (1983) 748.

[126] **properties of Group III Nitrides**, edited by J. H. Edgar (EMIS, London, (1994).

[127] B. Bouhafs, H. Aourag, M. Ferhat and M. Certier, J. *Phys.: Cond. Matter*, **11** (1999) 5781.

[128] B. Bouhafs, H. Aourag, and M. Certier, J. *Phys.: Cond. Matter*, **12** (2000) 4655.

[129] H. Meradji, S. Darbalia, S. Ghemid, H. Belkhir, B. Bouhafs, and A. Tadjer, *Phys. Stat. Solidi* (b) **241** (2004) 2881.

[130] Ramos LE, Teles LK, Scolfaro LMR, Castineira JLP, Rosa AL,Leite JR B **63** (2001) *Phys Rev*:165210

[131] P. Mori- Sanchez, A. M. Perdas, and V. Luana, *Phys. Rev* B**63** (2001)125103.

[132] P. Kocinski and M. Zbroszyk, *Semicond. Science and Technol*. **10**, 1452 (1995).

[133] F. D. Murnaghan, *Proc. Natl. Acad. Sci. U. S. A*. **30** (1944)244.

[134] R. W. Godby, M. Schl¨ uter, and L. J. Sham, *Phys. Rev*. B **37** (1988)10159.

[135] Q. Guo and A. Yoshida, Jpn. J. *Appl. Phys*. Part1 (**33**) (1994) 2453.

[136] J. Serrano, A. Rubio, E. Hern´ andez, A. Mu˜ noz, and A. Mujica, *Phys. Rev*. B **62** (2000)16612.

[137] A. Zoroddu, F. Bernardini, P. Ruggerone, and V. Fiorentini, *Phys. Rev*. B **64** (2001)045208.

[138] A. F. Wright and J. S. Nelson, *Phys. Rev*. B **51** (1995)7866.

[139] A. Mu¨ noz and K. Kunc, J. *Phys.: Condens. Matter* **5** (1993) 6015.

[140] D. H. Chow, H. L. Dunlap, W. Williamson, S. Enquist, B. K. Gilbert, S. Subramaniam, P. M. Lei, and G. H. Bernstein, *IEEE Electron Device Lett.***17** (1996)69.

[141] A. Mu¨ noz and K. Kunc, J. *Phys.: Condens. Matter* **5** (1993) 6015.

[142] M. Buongiorno Nardelli, K. Rapcewicz, E. L. Briggs, C. Bungaro, J. Bern-holc, in III-V Nitrides, edited by F. A. Ponce, T. D. Moustakas, I. Akasaki, and B. A. Monemar, MRS Symposia Proceedings No. 449 (*Materials Re-search Society, Pittsburgh*, (1997), p. **893.**

[143] K. Karch and F. Bachstedh, *Phys. Rev*. B **56** (1997) 7404.

J. P. Loehr and D. N. Talwar, *Phys. Rev*. B **55** (1997) 4353.

[144] Chan, X. M. Meng, and S. T. Lee, *Appl. Phys. Lett*. **85** (2004) 1344.

[145] **Semiconductors - Basic Data**, edited by: O. Madelung, (Berlin; Springer, 1996). ISBN 3-540-60883-4.

[146] R. M. Wentzcovitch, M. L. Cohen, and P. K. Lam, *Phys. Rev*. B **36** (1987) 6058.

[147] F. Bassani and M.Yoshimine, *Phys. Rev*. **130** (1963) 20.

[148] G. C. Osbourn and D. L. Smith, *Phys. Rev*. B **19** (1979)2124 D. R. Wiff and keown, J. *Chem. Phys*. **47** (1967) 3113.

[149] F. P. Bundy and R. H.Wentorf, J. *Chem. P hys*. **38** (1963) 1144.

[150] M. van Schilfgaarde, A. Sher, and A. B. Chen, J. *Cryst. Growth* **178**, (1997) 8.

[151] L. E. Ramos, L. K. Teles, L. M. R. Scolfaro, J. L. P.m Castineira, A. L.Rosa, and J. R. Leite, *Phys. Rev*. B **6**3, 165210 (2001).

[152] H. C. Hwang and J.Henkel*, Phys. Rev*. B **17** (1978) 4100.

[153] L.Kleinman and J.C. Phillips, *Phys. Rev*117 (1960) 460. R. Dovesi, C. Pisani, C. Roetti, and P. Dellarole, *Phys. Rev*. B **24** (1981) 4170.

[154] D. R. Wiff and R. Keown, J. *Chem. Phys*. 47, 3113 (1967).

[155] L. A. Hemstreet, Jr. and C.Y. Fong, *Phys. Rev*. B**6** (1972) 1464.

[156] M. Z. Huang and W. Y. Ching, J. *Phys. Chem. Solids Vol*. **46** (1985) 977.

[157] R. Archer, R. Y. Koyama, E. E. Loebner, and R. C. Lucas, *Phys. Rev. Lett.* **12** (1964) 538.

[158] F. Bloch, Z. *Physik*, **52**, (1928) 555.

[159] P. Blaha, K. Schwarz, G.K.H. Madsen, D. Kvasnicka, J. Luitz,*WIEN2K, An Augmented-Plane-Wave + Local Orbitals Program*

for Calculating Crystal Properties, Karlheinz Schwarz, Techn. Wien, Austria, 2001, ISBN 3-9501031-1-2.

[160] J. E. Bernard, A. Zunger, *Phys. Rev*. B **34,** (1986) 5992.

[161]L. Vegard, *Z. Phys*. **5**, 17 (1921)

[162]   F. El Haj Hassan [a], H. Akbarzadeh [b] *Materials Science and Engineering* B **121** (2005) 170–177.

[163] Rezek Mohammad and Senay Katırcıoglu present submitted to *Journal of Physics and Chemistry of Solid* (2008).

جامعة النجاح الوطنية

كلية الدراسات العليا

حساب الترتيب الالكتروني للمخاليط الثلاثية $B_xIn_{1-x}N$ و $B_xGa_{1-x}N$ و BN_xP_{1-x} في حالة التركيب كبريت الخارصين

إعداد

بسيمة دعاس فريد زبيدة

إشراف

د. موسى الحسن

د. رزق استيته

قدمت هذه الأطروحة استكمالا لمتطلبات نيل درجة الماجستير في الفيزياء بكلية الدراسات العليا في جامعة النجاح الوطنية في نابلس فلسطين.

2008

حساب الترتيب الالكتروني للمخاليط الثلاثية $B_xIn_{1-x}N$ و $B_xGa_{1-x}N$, و BN_xP_{1-x} في حالة التركيب كبريت الخارصين

إعداد

بسيمة دعاس فريد زبيدة

إشراف

د. موسى الحسن

د. رزق استيته

الملخص

تتحدث هذه الأطروحة عن طريقة الجهد المزبد التام ذو الموجات المستوية بالاستعانة بالشيفرة ($Wien2k-code$) من خلال نظرية الكثافة مستخدمين نظرية التدرج العام لتحرى التركيب الالكتروني و الخصائص الحيوية من المجموعة الثالثة (In, B, Ga) و المجموعة الخامسة (N, B). ومخاليطها في حالة التركيب البلوري لكبريتات الخارصين (ZnS).

الدراسة الحالية أظهرت إن المركبات GaN, InN بتركيبها الحالي تمتلك طاقة فجوة مباشرة بينما المركبات التالية BN, BP تمتلك طاقة فجوة غير مباشرة. إن قاع حزمة نطاق التوصيل لهذه المركبات تقع عند نقطة التماثل جاما إلا المركب BP, BN فإنها تقع على امتداد الخط بين جاما و اكس.

في هذا العمل أيضاً تم دراسة طاقة الفجوة للمخاليط $B_xIn_{1-x}N$ $B_xGa_{1-x}N$ و BN_xP_{1-x} عند التراكيز (0.25 0.50 0.75).

لقد وجدنا المخاليط $B_xGa_{1-x}N$ تمتلك أكبر تحدب في فجوة الطاقة لتراكيزها المختلفة.